Atmos. Chem. Phys., 17, 12361–12378, 2017
https://doi.org/10.5194/acp-17-12361-2017

Atmospheric Chemistry and Physics
Open Access
EGU

Fast heterogeneous N_2O_5 uptake and $ClNO_2$ production in power plant and industrial plumes observed in the nocturnal residual layer over the North China Plain

Zhe Wang[1], Weihao Wang[1], Yee Jun Tham[1,a], Qinyi Li[1], Hao Wang[2], Liang Wen[2], Xinfeng Wang[2], and Tao Wang[1]

[1]Department of Civil and Environmental Engineering, The Hong Kong Polytechnic University, Hong Kong, China
[2]Environment Research Institute, Shandong University, Jinan, China
[a]now at: Department of Physics, University of Helsinki, Helsinki, Finland

Correspondence to: Zhe Wang (z.wang@polyu.edu.hk) and Tao Wang (cetwang@polyu.edu.hk)

Received: 23 May 2017 – Discussion started: 29 May 2017
Revised: 23 August 2017 – Accepted: 16 September 2017 – Published: 17 October 2017

Abstract. Dinitrogen pentoxide (N_2O_5) and nitryl chloride ($ClNO_2$) are key species in nocturnal tropospheric chemistry and have significant effects on particulate nitrate formation and the following day's photochemistry through chlorine radical production and NO_x recycling upon photolysis of $ClNO_2$. To better understand the roles of N_2O_5 and $ClNO_2$ in the high-aerosol-loading environment of northern China, an intensive field study was carried out at a high-altitude site (Mt. Tai, 1465 m a.s.l.) in the North China Plain (NCP) during the summer of 2014. Elevated $ClNO_2$ plumes were frequently observed in the nocturnal residual layer with a maximum mixing ratio of 2.1 ppbv (1 min), whilst N_2O_5 was typically present at very low levels (< 30 pptv), indicating fast heterogeneous N_2O_5 hydrolysis. Combined analyses of chemical characteristics and backward trajectories indicated that the $ClNO_2$-laden air was caused by the transport of NO_x-rich plumes from the coal-fired industry and power plants in the NCP. The heterogeneous N_2O_5 uptake coefficient (γ) and $ClNO_2$ yield (ϕ) were estimated from steady-state analysis and observed growth rate of $ClNO_2$. The derived γ and ϕ exhibited high variability, with means of 0.061 ± 0.025 and 0.28 ± 0.24, respectively. These values are higher than those derived from previous laboratory and field studies in other regions and cannot be well characterized by model parameterizations. Fast heterogeneous N_2O_5 reactions dominated the nocturnal NO_x loss in the residual layer over this region and contributed to substantial nitrate formation of up to 17 $\mu g\,m^{-3}$. The estimated nocturnal nitrate formation rates ranged from 0.2 to 4.8 $\mu g\,m^{-3}\,h^{-1}$ in various plumes, with a mean of 2.2 $\pm 1.4\,\mu g\,m^{-3}\,h^{-1}$. The results demonstrate the significance of heterogeneous N_2O_5 reactivity and chlorine activation in the NCP, and their unique and universal roles in fine aerosol formation and NO_x transformation, and thus their potential impacts on regional haze pollution in northern China.

1 Introduction

Nitrogen oxides ($NO_x = NO + NO_2$) play central roles in the oxidative capacity of the atmosphere and photochemical air pollution. Dinitrogen pentoxide (N_2O_5) is an important reactive intermediate in the oxidation of NO_x and exists in rapid thermal equilibrium with nitrate radical (NO_3) formed via the reaction between NO_2 and O_3. The heterogeneous hydrolysis of N_2O_5 has been recognized as a key step in nocturnal NO_x removal and can affect regional air quality by regulating the reactive nitrogen budget and nitrate aerosol formation (e.g., Brown et al., 2006; Abbatt et al., 2012). The heterogeneous reaction of N_2O_5 on and within atmospheric aerosols, fog, or cloud droplets produces soluble nitrate (HNO_3 or NO_3^-) and nitryl chloride ($ClNO_2$) when chloride is available in the aerosols (Finlayson-Pitts et al., 1989).

$$N_2O_5 + H_2O(het) \rightarrow 2HNO_3(aq) \quad \text{(R1)}$$

$$N_2O_5 + Cl(het) \rightarrow NO_3(aq) + ClNO_2 \quad \text{(R2)}$$

The rate coefficient of the heterogeneous N_2O_5 reactions is governed by the available reaction surface and N_2O_5 reaction

probability (also known as the uptake coefficient $\gamma_{N_2O_5}$), and it can be described by the following expression when the gas-phase diffusive effect is negligible.

$$k(N_2O_5)_{het} = \frac{1}{4} c_{N_2O_5} \gamma_{N_2O_5} S_a \quad (1)$$

Here, $c_{N_2O_5}$ is the mean molecular speed of N_2O_5, and S_a is the aerosol (or cloud) surface area density. The yield of $ClNO_2$ (ϕ) is defined as the amount of $ClNO_2$ formed per loss of N_2O_5, representing the fraction to $ClNO_2$ formation. Hence, the net reaction of Reactions (R1) and (R2) can be written as follows:

$$N_2O_5 + (H_2O \text{ or } Cl)\,(het) \rightarrow (2-\phi)NO_3^-\,(aq) + \phi ClNO_2. \quad (R3)$$

The $\gamma_{N_2O_5}$ has been experimentally measured on various types of aerosols surfaces (including sulfate, nitrate, black carbon, organic carbon, organic coating sulfate, sea salts, and dust) in the laboratory, and different parameterizations based on aerosol composition have been proposed in varying degrees of complexity (e.g., Evans and Jacob, 2005; Anttila et al., 2006; Davis et al., 2008; Bertram and Thornton, 2009; Griffiths et al., 2009; Riemer et al., 2009; Roberts et al., 2009; Simon et al., 2009; Foley et al., 2010; Chang et al., 2011; Ammann et al., 2013; Tang et al., 2014). Recently, field studies have been carried out to measure ambient N_2O_5 and to derive $\gamma_{N_2O_5}$ from atmospheric observations (e.g., Bertram et al., 2009b; Brown et al., 2009, 2016; Morgan et al., 2015; Chang et al., 2016; Phillips et al., 2016). These field-derived/measured $\gamma_{N_2O_5}$ values were found to vary considerably, and the observed range was found to be significantly larger than that from laboratory studies using synthetic aerosols (Chang et al., 2011; Phillips et al., 2016). Furthermore, inconsistencies between $\gamma_{N_2O_5}$ values derived from field measurements and parameterizations were observed in some locations, which implies that $\gamma_{N_2O_5}$ has a complex dependence on the aerosol composition, physicochemical characteristics, and environmental parameters (Chang et al., 2011, and references therein). Similarly, for the $ClNO_2$ yield, the field-determined values exhibited significant variability, ranging from 0.01 to close to unity (Thornton et al., 2010; Riedel et al., 2013; Wagner et al., 2013; Phillips et al., 2016), which could not be well reproduced (exhibiting a 10-fold difference in some cases) by parameterization based on only aerosol chloride and water content (Wagner et al., 2013; X. Wang et al., 2017). There are only few studies on the determination of ϕ from field measurement, and the possible effects of real atmospheric aerosols (including organic composition, mixing state, and chloride partitioning between particle sizes) have not been well characterized (Mielke et al., 2013; Phillips et al., 2016). This incomplete understanding suggests the necessity of more field measurements of γ and ϕ in various environments to facilitate the validation and construction of parameterizations suitable for use in air quality models.

$ClNO_2$ formed from nocturnal heterogeneous N_2O_5 uptake can potentially affect the atmospheric oxidative capacity via the production of highly reactive chlorine radicals (Cl) and the recycling of NO_x after photolysis (Simpson et al., 2015). Elevated $ClNO_2$ mixing ratios were firstly observed in several polluted coast regions (for instance, the coasts of Texas and California, and the Los Angeles Basin), resulting from the strong emission of NO_x and abundant chloride from sea salt aerosols (Osthoff et al., 2008; Riedel et al., 2012; Mielke et al., 2013; Tham et al., 2014). Recently, significant $ClNO_2$ production was also observed in some inland areas (such as Colorado, Hessen, and Alberta), with a mixing ratio of up to several hundreds of pptv or even exceeding 1.0 ppbv (e.g., Thornton et al., 2010; Mielke et al., 2011, 2016; Phillips et al., 2012; Riedel et al., 2013; Faxon et al., 2015). Anthropogenic sources of chlorine including coal combustion in power plants, industries, and biomass burning may potentially facilitate $ClNO_2$ production (Riedel et al., 2013). The highest $ClNO_2$ mixing ratio yet reported (4.7 ± 0.8 ppbv, 1 min average) was recently observed in the regional plumes at a mountaintop site in southern China, indicating the importance of $N_2O_5/ClNO_2$ chemistry in polluted environments (Wang et al., 2016).

Large anthropogenic emissions of NO_x and increasing O_3 concentrations have been reported in many urban cluster regions in China (Wang et al., 2006; T. Wang et al., 2017). Hence, in these regions, nocturnal nitrogen chemistry may be particularly important in the transformation of NO_x and the subsequent effects on daytime photochemistry and secondary aerosol formation. In the areas downwind of Beijing and Shanghai, high concentrations of particulate nitrate (up to 40 $\mu g\,m^3$) have been observed and attributed to heterogeneous N_2O_5 uptake on acidic aerosols (Pathak et al., 2009, 2011). During a more recent field study in a rural site in the North China Plain (NCP), elevated fine nitrate concentrations were observed at night and in the early morning, with hourly maxima of up to 87.2 $\mu g\,m^{-3}$ and a 30 % contribution to $PM_{2.5}$, which was mainly attributed to the heterogeneous hydrolysis of N_2O_5 (Wen et al., 2015). Active heterogeneous N_2O_5 chemistry has been recently characterized in both rural and urban areas of the NCP via direct measurements of N_2O_5 and $ClNO_2$. Rapid heterogeneous N_2O_5 loss and efficient $ClNO_2$ production were observed, with a maximum $ClNO_2$ mixing ratio of 2.07 ppbv at Wangdu and 0.77 ppbv at Jinan (Tham et al., 2016; X. Wang et al., 2017). Moreover, sustained $ClNO_2$ peaks were observed after sunrise in the region, and the downward mixing of $ClNO_2$-rich air in the residual layer was proposed to be the cause of morning peaks (Tham et al., 2016). To confirm these findings and better characterize the chemistry of $N_2O_5/ClNO_2$ and their impacts on regional air quality, it is of great interest to conduct direct field measurements of $N_2O_5/ClNO_2$ in the polluted residual layer.

In the present study, we measured the concentrations of N_2O_5, $ClNO_2$, and related species at a mountaintop site in

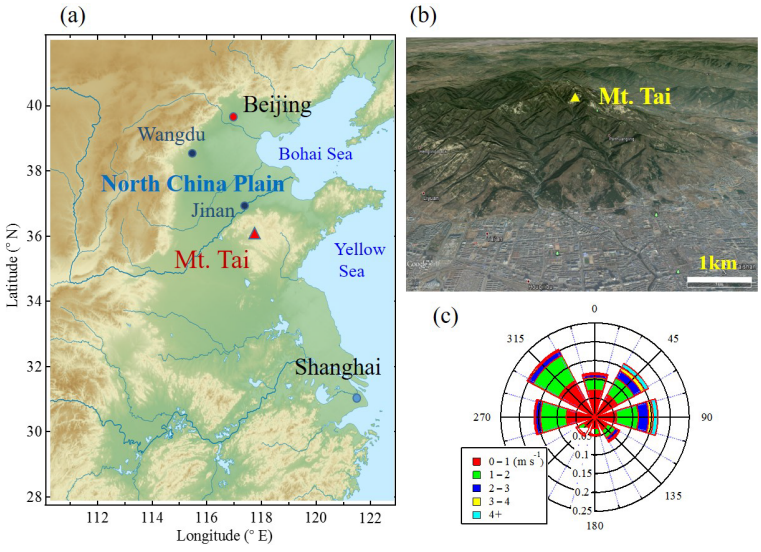

Figure 1. **(a)** Map of northern China showing the location of the mountaintop measurement site (Mt. Tai) in the North China Plain, **(b)** expanded topographic view of Mt. Tai and surrounding areas, and **(c)** a wind rose for the study period of summer 2014.

the NCP during the summer of 2014 and characterized the nighttime nitrogen chemistry within the residual layer over a polluted region of northern China. We examined the frequently intercepted $ClNO_2$-rich plumes at this high-elevation site and investigated nocturnal N_2O_5 reactivity to determine the heterogeneous N_2O_5 uptake coefficients and $ClNO_2$ yields in a variety of air masses, which were also compared to parameterizations utilized in existing models. The effects of heterogeneous N_2O_5 chemistry on particulate nitrate formation and nocturnal NO_x loss were then evaluated based on the observation data.

2 Methodology

2.1 Field study site

The measurement site was located on Mount Tai (36.25° N, 117.10° E, 1465 m a.s.l. – above sea level) in Shandong Province, China. Mt. Tai is located between the two most developed regions in China (Jing–Jin–Ji and the Yangtze River Delta), and its peak (1545 m a.s.l.) is the highest point within the NCP. Figure 1 shows the location of the measurement site in relation to the surrounding topography. Mt. Tai is 230 km away from the Bohai and Yellow seas, and the cities of Tai'an and Jinan (the capital of Shandong Province) are located 15 km south and 60 km north of the measurement site, respectively. The altitude of the measurement site is near the top of the boundary layer in the daytime during the summer and is typically in the residual layer or, occasionally, in the free troposphere at night. This mountaintop site has been previously used in many atmospheric chemistry field studies (e.g., Gao et al., 2005; Wang et al., 2011; Guo et al., 2012; Sun et al., 2016). Previous studies at this site indicated that the site is regionally representative without significant local anthropogenic emissions and affected by the regional aged air masses and occasional combustion plumes from fossil fuel or biomass in the region (e.g., Zhou et al., 2009; Wang et al., 2011; Guo et al., 2012). Intensive measurements were performed from 24 July to 27 August 2014. During this period, the prevailing winds originated from the northeast and northwest. Shandong province is the largest producer of thermal power in China, and dozens of coal-fired industry and power plants are situated within a radius of 200 km from the mountain site.

2.2 Instrumentation

N_2O_5 and $ClNO_2$ were measured concurrently using iodide ion chemical ionization mass spectrometry (CIMS) with a quadrupole mass spectrometer (THS Instruments Inc., USA). The principle and detailed calibration of this CIMS system have been described previously by Wang et al. (2016) and Tham et al. (2016). The same configuration was used in the present study. Briefly, N_2O_5 and $ClNO_2$ were detected as $I(N_2O_5)^-$ and $I(ClNO_2)^-$ clusters via reaction with iodide ions (I^-), which were generated from a mixture of CH_3I (0.3 % in volume) and N_2 using an alpha radioactive source, ^{210}Po (NRD, P-2031-2000). The inlet was installed $\sim$ 1.5 m above the roof of a single-story building, and the sampling line was a 5.5 m PFA-Teflon tubing (1/4 in o.d.) which was replaced daily in the afternoon before sunset and washed in the ultrasonic bath to minimize wall loss caused by deposited particles (Wang et al., 2016). A small proportion (1.7 SLPM) of total sampling flow ($\sim$ 11 SLPM) was diverted to the CIMS system to reduce the residence time of the air samples in the sampling line. A standard addition of N_2O_5 into

the ambient inlet was performed before and after the tubing replacement to monitor the transmission efficiency, and this practice limited the loss of N_2O_5 in the inlet to $< 10\,\%$ in the "clean" tubing and about 30 % in the next afternoon. Manual calibrations of N_2O_5 and $ClNO_2$ were conducted daily to determine the instrument sensitivity, the average of which was 2.0 ± 0.6 for N_2O_5 and $2.2 \pm 0.6\,\mathrm{Hz\,pptv^{-1}}$ for $ClNO_2$, respectively, during the observation period. The N_2O_5 standard was synthesized online from the reaction between NO_2 and O_3, and the produced N_2O_5 was determined from the decrease in NO_2 (Wang et al., 2014). This method has been validated with a cavity ring-down spectrometer (CRDS) measurement in a previous campaign (Wang et al., 2016). The $ClNO_2$ was produced by passing a known concentration of N_2O_5 through a NaCl slurry, assuming unity conversion efficiency (Roberts et al., 2009) and negligible $ClNO_2$ loss in the system (Wang et al., 2016). The field background was determined by passing the ambient sample through a filter packed with activated carbon, with average levels of 7.8 ± 1.9 and $6.0 \pm 1.6\,\mathrm{Hz}$ for N_2O_5 and $ClNO_2$, respectively. The reported concentrations were derived by subtracting the background levels. The detection limit was 4 pptv for both N_2O_5 and $ClNO_2$ (2σ, 1 min averaged data), and the uncertainty of the nighttime measurement was estimated to be $\pm 25\,\%$ (Tham et al., 2016).

The related trace gases and aerosol compositions were also measured concurrently during the campaign. All of the instruments were used in our previous field studies, and the setup, precision, and accuracies of these instruments were described previously (Wen et al., 2015; Tham et al., 2016; Wang et al., 2016; X. Wang et al., 2017). Briefly, NO and NO_2 were measured using a chemiluminescence analyzer equipped with a blue-light converter (TEI, Model 42I-TL). Total gaseous reactive nitrogen (NO_y) was determined using a chemiluminescence analyzer with an external molybdenum oxide (MoO) catalytic converter (TEI, Model 42CY) with an inlet filter. The NO_y described here is different from that in previous reports (Tham et al., 2016; Wang et al., 2016), because the particulate nitrate was not included but removed by the filter in the present study. O_3, SO_2, and CO were measured using the ultraviolet photometry, pulsed-UV fluorescence, and IR (infrared) photometry techniques (TEI, Model 49I, 43C, and 48C), respectively. Zero and span calibrations for trace gases were performed weekly during the campaign. Water-soluble ionic compositions of $PM_{2.5}$ (including NH_4^+, Na^+, Ca^{2+}, Mg^{2+}, Cl^-, SO_4^{2-}, and NO_3^-) were measured hourly by a monitor for aerosols and gases in ambient air (MARGA ADI 2080, Applikon–ECN) using online ion chromatography.

The particle number and size distribution (5 nm to 10 µm) were measured using a wide-range particle spectrometer (WPS, model 1000XP, MSP Corporation, USA). The particle diameters were corrected for particle hygroscopicity to determine the actual ambient aerosol surface density, and the wet diameters were calculated using growth factors from a size-resolved κ-Köhler function obtained in a rural site in the NCP (Ma et al., 2016; Tham et al., 2016). The uncertainties associated with the aerosol surface area determination was estimated to be around 30 % (Liu et al., 2010; Tham et al., 2016). Meteorological data, including temperature, relative humidity (RH), wind vectors, and photolysis frequency of NO_2 (J_{NO_2}), were measured by an automated meteorological station (PC-4, JZYG) and a filter radiometer (Metcon, Germany). In addition, a Lagrangian particle dispersion model, Hybrid Single-Particle Lagrangian Integrated Trajectory (HYSPLIT) model (Draxler and Hess, 1998; Wang et al., 2016), driven by high spatial and temporal meteorological fields from the Weather Research and Forecasting (WRF) Model, was used to investigate potential source regions of the air masses intercepted at the measurement site. The HYSPLIT model was run 12 h backward with 2500 particles released at the measurement site. Detailed parameterization and setup of the HYSPLIT and WRF models were previously described by Wang et al. (2016) and Tham et al. (2016).

3 Results and discussion

3.1 Overview of N_2O_5 and $ClNO_2$ measurement

The temporal variations of $ClNO_2$, N_2O_5, related trace gases, aerosol properties, and selected meteorological parameters during the field study at Mt. Tai are depicted in Fig. 2. Overall, the observed mixing ratios of $ClNO_2$ were higher than those of N_2O_5 and exhibited significant variations. The average mixing ratios of N_2O_5 and $ClNO_2$ were 6.8 ± 7.7 and 54 ± 106 pptv, respectively. The maximum mixing ratio of N_2O_5 (167 pptv) was observed at 21:00 LT on 26 August 2014, and most of the other nights during the observation period exhibited peak N_2O_5 mixing ratios below 30 pptv. The average nighttime mixing ratios of O_3 and NO_2 were 77 and 3.0 ppbv, respectively, with an average nitrate radical production rate $p(NO_3)$ of $0.45 \pm 0.40\,\mathrm{ppbv\,h^{-1}}$, which is indicative of potentially active NO_3 and N_2O_5 chemistry during the study period. However, the low N_2O_5 mixing ratios observed during most of the nights suggest a rapid loss of N_2O_5, which is consistent with the observed high aerosol surface area (S_a), which varied from ~ 100 to $7800\,\mu\mathrm{m^2\,cm^{-3}}$ with a mean value of $1440\,\mu\mathrm{m^2\,cm^{-3}}$. The higher RH during nighttime and the frequent occurrence of clouds at the mountaintop site could also account for low N_2O_5 concentrations, because of the rapid heterogeneous loss of N_2O_5 on cloud droplets.

The highest $ClNO_2$ mixing ratio of 2065 pptv was observed on 8 August 2014, and on 8 of the 35 nights the peak $ClNO_2$ mixing ratios were higher than 500 pptv. The simultaneous increases of SO_2, NO_x, and CO with the $ClNO_2$ peaks suggest these air masses originated from coal combustion sources, such as industry and power plants, which will be further discussed in the next section. The elevated $ClNO_2$

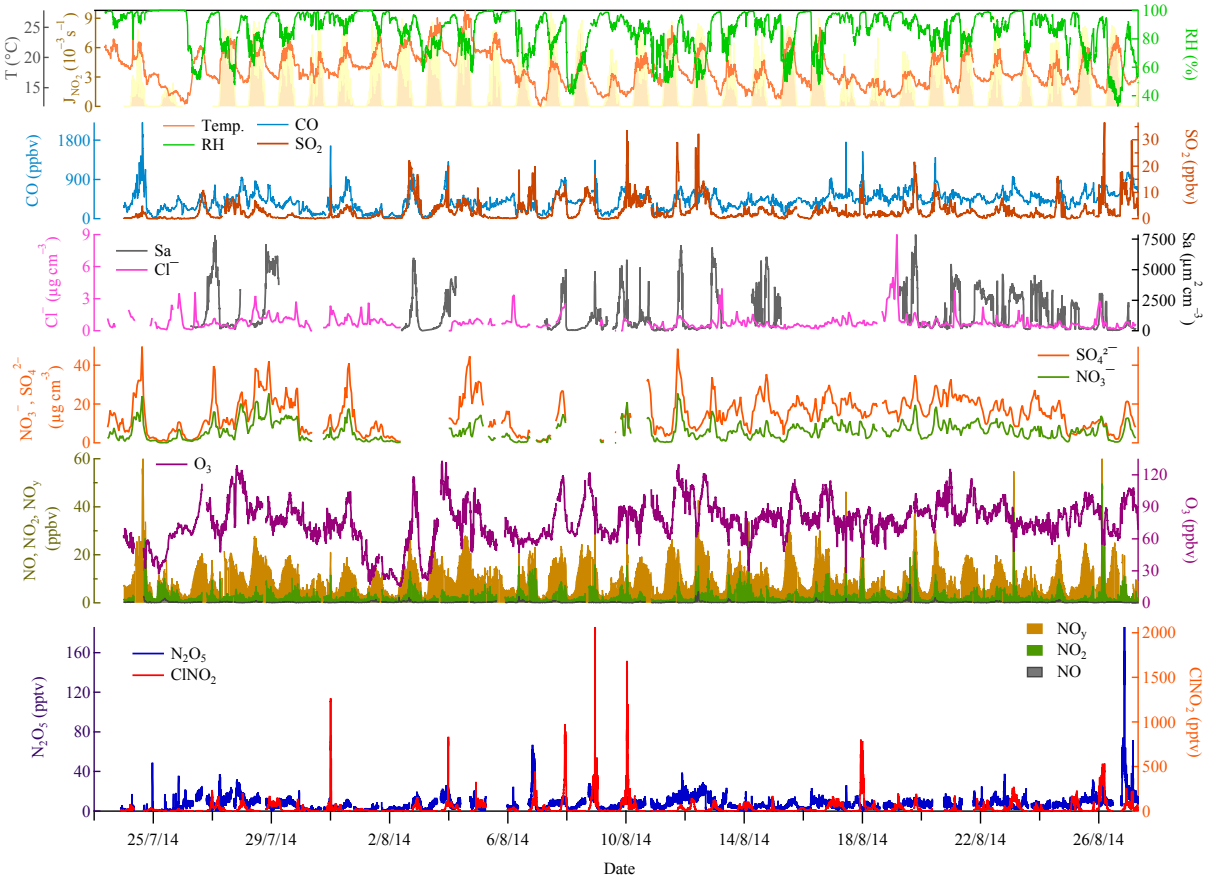

Figure 2. Time series for N_2O_5, $ClNO_2$, related trace gases, aerosol properties, and meteorological data measured at Mt. Tai from 24 July to 27 August 2014.

levels observed at Mt. Tai are similar to recent measurements at a surface rural site (Wangdu) in northern China (Tham et al., 2016) and a mountain site (Tai Mo Shan) in southern China (Wang et al., 2016) but are slightly higher than previous measurements conducted in coastal (e.g., Osthoff et al., 2008; Riedel et al., 2012; Mielke et al., 2013) and inland sites (e.g., Thornton et al., 2010; Phillips et al., 2012; Riedel et al., 2013) in other regions of the world. During the campaign at Mt. Tai, the average concentrations of aerosol sulfate and nitrate were 14.8 ± 9.0 and 6.0 ± 4.7 μg m^{-3}, accounting for 29.5 and 12.0 % of $PM_{2.5}$ mass, respectively. The aerosol organic-to-sulfate ratio, a parameter that potentially affects the uptake process (Bertram et al., 2009b), was 0.74 on average and much lower than those from studies mentioned above in Europe and the USA. Moreover, the nighttime averaged Cl^- concentration was 0.89 ± 0.86 μg cm^{-3}, and was an order of magnitude higher than Na^+, indicating abundant non-oceanic sources of chloride (e.g., from coal combustion and biomass burning in the NCP) (Tham et al., 2016), which could enhance the production of $ClNO_2$.

The mean diurnal variations of N_2O_5, $ClNO_2$, and other relevant chemical species during the study period are shown in Fig. 3. Ozone exhibited a typical diurnal pattern for a polluted mountaintop site (Sun et al., 2016), and it began to increase in the late morning and reached an afternoon peak of 88.6 (±16.6) ppbv, with a daily average rise of 24.4 ppbv. The average O_3 remained at elevated levels after sunset and did not begin to decrease until 22:00 LT, and NO_x exhibited a diel maximum of 6.1 ppbv before sunset, resulting in a peak in $p(NO_3)$ just before sunset and relatively high levels in the early night. Gaseous NO_y reached a maximum of 16.4 (±6.1) ppbv in the morning and remained stable at a high level during the daytime; the air masses were more aged during the daytime, as indicated by the persistent low NO_x/NO_y ratios (0.2–0.25). Small N_2O_5 peaks were observed immediately after sunset, resulting from the abundant O_3 and NO_2, and N_2O_5 was present at low levels near the detection limit of the CIMS throughout the rest of the night. $ClNO_2$ exhibited clear nighttime elevations resulting from the heterogeneous production after sunset and reached a diel maximum around midnight. The low N_2O_5 and high $ClNO_2$ concentrations observed at Mt. Tai are similar to the measurement at a rural surface site within the NCP (Tham et al.,

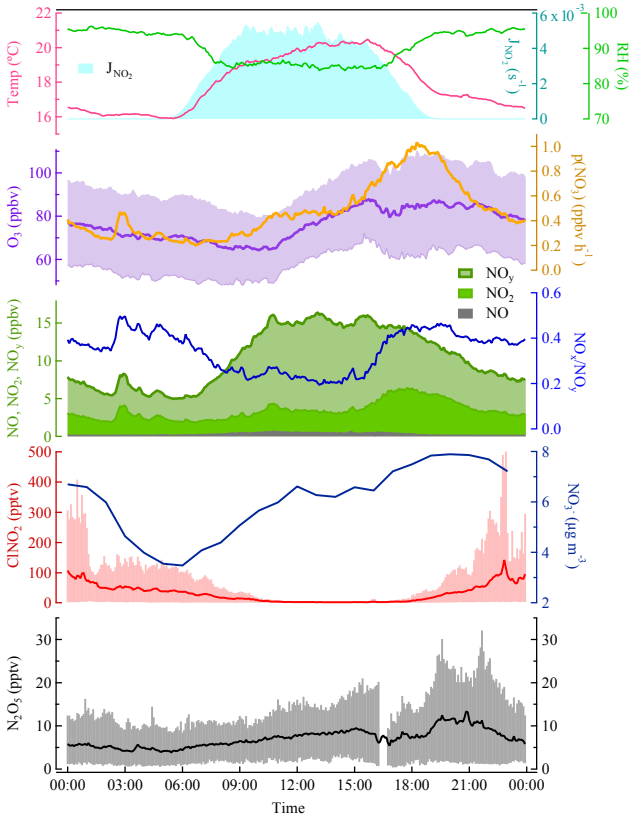

Figure 3. Diurnal variations of N_2O_5, $ClNO_2$, NO_x, NO_y, O_3, particulate nitrate, nitrate radical production rate $p(NO_3)$, and meteorological parameters during the study period at Mt. Tai. Shaded area in O_3 shows 2σ variation, and vertical bars in N_2O_5 and $ClNO_2$ represent 10–90th percentile ranges.

2016), suggesting rapid heterogeneous loss of N_2O_5 and production of $ClNO_2$ in this region.

It was also noted that a small N_2O_5 peak ($\sim$ 10 pptv) with larger variability was present in the early afternoon. A simplified photostationary analysis following Brown et al. (2005, 2016) was performed to predict the daytime steady-state N_2O_5 concentrations for the few cases with daytime peaks. The predicted concentrations all showed increasing trends in the afternoon, similar to the observation pattern. However, for individual cases, the predicted values around 15:00 LT were much lower than the observation under clean sky condition, but of the same magnitude as the observation for reduced photolysis and foggy conditions with higher NO_3 production rate (cf. Fig. S1 in the Supplement). Daytime N_2O_5 signals with few pptv have also been observed by a CRDS at a mountain site in southern China (Brown et al., 2016), where the concentrations were in accord with steady-state estimation in an average sense. Because daily maintenance and calibrations of the CIMS were usually performed during early afternoon periods, the limited daytime data in the present study were not sufficient to make clear whether there were any daytime interferences or sensitivity fluctuations. Thus, additional studies are needed to validate the daytime phenomenon and examine the potential reasons, and the following analysis in the present work will mostly focus on nocturnal processes.

3.2 High-$ClNO_2$ plumes from power plants and industry

As described above, several plumes with elevated $ClNO_2$ concentrations (> 500 pptv) were observed during the measurement period. Figure 4a illustrates the high-$ClNO_2$ case observed during the night of 30–31 July 2014. The $ClNO_2$ concentration peaked sharply at 1265 pptv, which was accompanied by a steep rise in the concentrations of SO_2, NO_x, and CO. The SO_2/NO_y ratio increased from $\sim$ 0.1 to 0.6 in the plume center, with a $\Delta SO_2/\Delta NO_y$ slope of 0.57, indicating the coal combustion source of the plume. The coincident increase in CO / NO_y ratio from $\sim$ 30 to 90 suggests that it likely originated from coal-fired industry facilities, such as cement and steel production plants, which is the largest emitting sector of CO in north China (Streets et al., 2006; Zhang et al., 2009). The 12 h backward particle dispersion trajectories calculated from the HYSPLIT model revealed that the air masses mostly moved slowly from the west and passed over the region with the cement and steel production industry and power plants before arriving at the measurement site. Figure 5a shows the highest $ClNO_2$ case (2065 pptv) observed on the night of 8 August 2014. The simultaneous increases in SO_2, NO_x, and CO concentrations, together with the higher SO_2/NO_y ratio ($\sim$ 0.5) compared to that outside of the plume ($\sim$ 0.1) and the campaign average (0.24), again indicate the coal combustion origin of the plume. The relatively lower CO / NO_y ratio ($\sim$ 50) possibly suggests the plume affected by power plant emission, as shown by the derived backward particle dispersion trajectories. Table 1 summarizes the chemical characteristics of the eight cases of high-$ClNO_2$ plumes from power plants and industry during the study period. In these cases, the average SO_2 mixing ratios ranged from 2.3 to 18.7 ppbv, and the maximum $ClNO_2$ and N_2O_5 mixing ratios ranged from 534 to 2065 pptv and 7.3 to 40.1 pptv, respectively, with corresponding $ClNO_2/N_2O_5$ ratios of 25 to 118. The mixing ratios for O_3 and NO_2 ranged from 60 to 106 ppbv and 2.8 to 11.8 ppbv, respectively, resulting in high $p(NO_3)$ values of 0.60 to 1.59 ppbv h^{-1}. The aerosol chloride concentration ranged from 1.01 to 2.34 $\mu g\ cm^{-3}$, which was higher than the nighttime average (0.89 $\mu g\ cm^{-3}$) and conducive to $ClNO_2$ production from Reaction (R3).

NO_x emissions from the coal combustion sources contain abundant NO, which is oxidized rapidly to NO_2 by ambient O_3. Thus, the anti-correlation between O_3 and NO_2 within the observed plumes (cf. Figs. 4b and 5b) can be another indicator of the large combustion sources (such as coal-fired power or industry plants). Furthermore, the slope of a plot of O_3 vs. NO_2 for nighttime plumes can be considered as an

Table 1. Chemical characteristics of coal-fired power plant and industrial plumes exhibiting high levels of $ClNO_2$ observed at Mt. Tai during the summer of 2014.

Date	Duration	N_2O_5 (pptv)		$ClNO_2$ (pptv)		O_3	NO_x	NO_x/ NO_y	ΔSO_2/ ΔNO_y^a	ΔCO/ ΔNO_y^b	Cl^- ($\mu g\,cm^{-3}$)	t_{plume}	ϕ_{ClNO_2}
		Mean	Maximum	Mean	Maximum								
30–31 Jul	23:40–00:45	5.9	14.2	528	1265	70	6.5	0.49	0.57	83	2.34	3.2	0.57
3–4 Aug	23:30–00:00	20.1	23.8	506	833	106	2.8	0.22	2.43	108	NA[c]	4.9	0.64
7 Aug	21:30–23:30	10.5	14.9	606	976	91	5.8	0.36	1.36	50	2.24	5.5	0.35[d]
8 Aug	22:00–23:10	11.0	15.1	841	2065	76	8.5	0.45	0.65	45	NA	2.1	0.90
8–9 Aug	23:40–01:15	6.8	12.6	315	599	77	4.3	0.41	0.54	85	NA	4.4	0.23
10 Aug	00:00–02:00	10.5	15.5	692	1684	72	6.2	0.43	1.67	50	1.10	4.6	0.55
17–18 Aug	22:00–01:30	3.5	7.7	409	802	60	9.5	0.55	0.48	33	1.01	4.6	0.26[d]
25–26 Aug	00:00–05:00	12.1	40.1	301	534	74	11.8	0.62	2.10	NA	1.88	3.0	0.20

[a] Slope of SO_2 vs. NO_y in plumes; the overall slope for entire campaign was 0.31 with r^2 of 0.31. [b] Same as previous note but with the campaign overall slope of 15.7 and r^2 of 0.23. [c] Data not available in the case. [d] For t_{plumes} longer than the nocturnal processing period since sunset, the time since sunset was used in the $ClNO_2$ yield calculation.

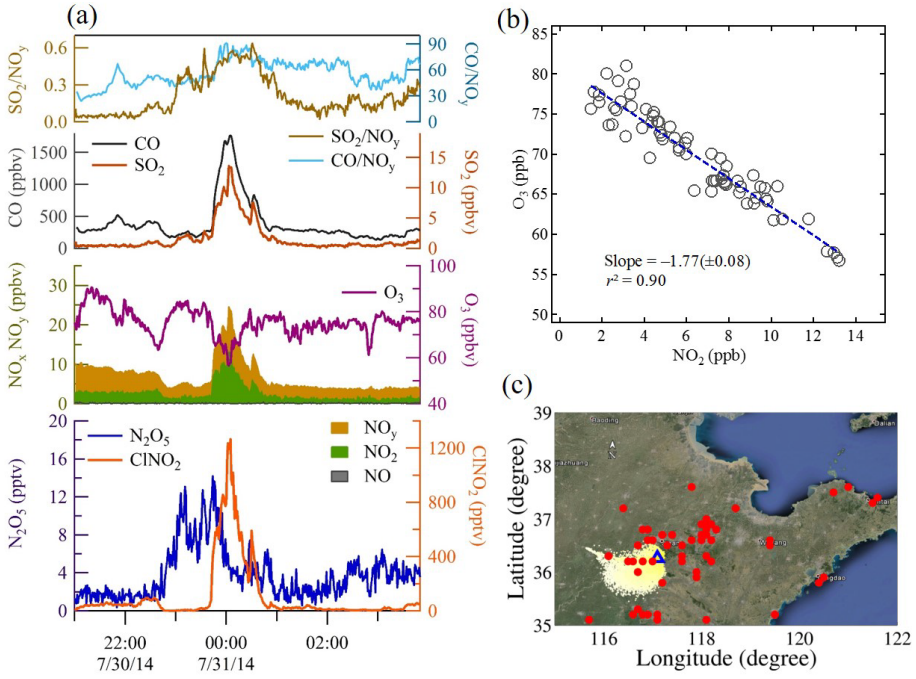

Figure 4. (a) Time series for $ClNO_2$, N_2O_5, and related trace gases observed within the high-$ClNO_2$ plume from power plants and industry during the night of 30–31 July 2014. **(b)** Plot of O_3 vs. NO_2 concentrations for the plume; plume age was determined from the plot using Eq. (2). **(c)** 12 h HYSPLIT backward particle dispersion image depicting air masses arriving at the measurement site (blue triangle) at the time of the plume, and red dots indicating the location of major coal-fired facilities in cement and steel production and power plants in the region.

approximate measure of the plume age, with the assumption of pseudo-first-order kinetics and when the input of NO_x is small compared to the excess O_3 (Brown et al., 2006). The estimated plume age can be determined as follows:

$$t_{plumes} \approx \ln(1 - S(m+1)) \,/\, \left(Sk\overline{O_3}\right), \quad (2)$$

where m is the derived slope, k is the rate coefficient for the reaction of NO_2 with O_3, $\overline{O_3}$ is the average O_3 concentration in the plume, and S is a stoichiometric factor that varies between 1 for dominant NO_3 loss and 2 for dominant N_2O_5 loss (Brown et al., 2006). In the present study, heterogeneous N_2O_5 uptake dominated the reactive nitrogen loss; therefore, $S = 2$ was used in the calculation. The plume ages for the 30–31 July and 8 August cases were calculated to be 3.2 and 2.1 h, respectively, which are consistent with the moderate NO_x/NO_y ratios of 0.4–0.5 and comparable to those observed in nocturnal power plant plumes in the eastern coast of the USA (Brown et al., 2006, 2007). The slopes of O_3 vs. NO_2 in Figs. 4b and 5b steeper than -1.0 also indicate the further reactions of NO_2 with O_3, which favor the formation of NO_3 and N_2O_5. However, the N_2O_5 concentrations only showed a slight increase (Fig. 4 case) or no apparent

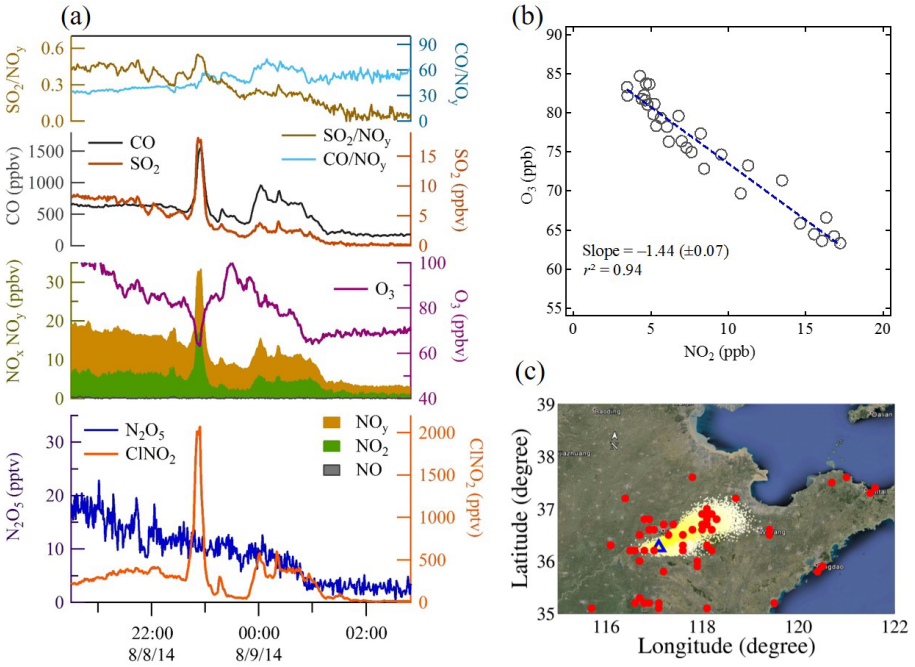

Figure 5. Same as Fig. 4 but for a plume observed during the night of 8–9 August 2014.

change (Fig. 5 case), in contrast to the significant increases in $ClNO_2$ and high $p(NO_3)$ values, which suggests rapid heterogeneous loss of N_2O_5 and significant $ClNO_2$ production during transport of these plumes from their sources.

The elevated $ClNO_2$ concentrations in the coal-fired power plant and industry plumes (here referred to collectively as coal-fired plumes) here are comparable to previous observations of power plant plumes via tower measurements in Colorado (Riedel et al., 2013) and at a mountain site in southern China (Wang et al., 2016), but the observed N_2O_5 within the plumes is significantly lower than those in other coal-fired plumes observed via aircraft, tower, and at mountain sites (Brown et al., 2007, 2016; Riedel et al., 2013). The previous measurement at a surface site in the NCP has observed sustained $ClNO_2$ peaks after sunrise, which was proposed to be the cause of the downward mixing of $ClNO_2$-rich air (estimated values of 1.7–4.0 ppbv) in the residual layer (Tham et al., 2016). In the present study, the frequent intercepts of coal-fired power plant and industrial plumes with elevated $ClNO_2$ concentrations at Mt. Tai, which was typically above the nocturnal boundary layer, affirm this hypothesis and provide direct evidence that significant $ClNO_2$ production occurred in the residual layer from the abundant nocturnal NO_x, chloride, and background O_3 over the NCP. The similar $ClNO_2$-laden air frequently observed at high-elevation sites in northern and southern China suggests ubiquitous $ClNO_2$ in the polluted residual layer and its importance in the daytime production of ozone in China (Tham et al., 2016; Wang et al., 2016). Moreover, the concurrent nitrate production from heterogeneous N_2O_5 reactions (cf. Reaction R3) may also contribute to the formation of haze pollution in these regions.

3.3 N_2O_5 reactivity and heterogeneous uptake coefficient

3.3.1 Reactivity of N_2O_5 and NO_3

The mixing ratios of N_2O_5 depend on the nitrate radical production rate and on the reactivity of N_2O_5 and NO_3, including the individual loss rates for N_2O_5 or NO_3 that contribute to the removal of the pair. N_2O_5 reactivity can be assessed using the inverse N_2O_5 steady-state lifetime, which is the ratio of $p(NO_3)$ to the observed N_2O_5 mixing ratios (e.g., Brown et al., 2006, 2009, 2016):

$$\tau(N_2O_5)^{-1} = \frac{p(NO_3)}{[N_2O_5]} \approx \frac{k(NO_3)}{K_{eq}[NO_2]} + k(N_2O_5)_{het}. \quad (3)$$

The steady-state inverse lifetime of N_2O_5, $\tau(N_2O_5)^{-1}$, is the sum of the N_2O_5 loss rate via heterogeneous loss ($k(N_2O_5)_{het}$) and NO_3 reactions with volatile organic compounds (VOCs) ($k(NO_3)$) with a ratio of $K_{eq}[NO_2]$. K_{eq} is the temperature-dependent N_2O_5–NO_3 equilibrium coefficient. High N_2O_5 reactivity was observed in the present study, with average nighttime $\tau(N_2O_5)^{-1}$ of $1.41 \times 10^{-2}\,s^{-1}$ before midnight and $1.30 \times 10^{-2}\,s^{-1}$ after midnight, corresponding to a nighttime N_2O_5 lifetime of 1.2–1.3 min. This rapid N_2O_5 loss rate is comparable to the results from surface measurements in both urban and rural sites in the NCP (Tham et al., 2016; X. Wang et al., 2017). However, this loss rate is

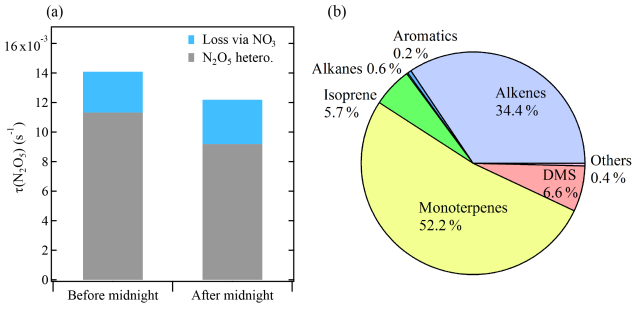

Figure 6. **(a)** Fractions of N_2O_5 loss rate coefficients through NO_3 loss and the heterogeneous reaction of N_2O_5 before (19:00–24:00 LT) and after midnight (01:00–05:00 LT); **(b)** pie chart showing the average nighttime contributions of different categories of VOCs to NO_3 reactivity during the study period.

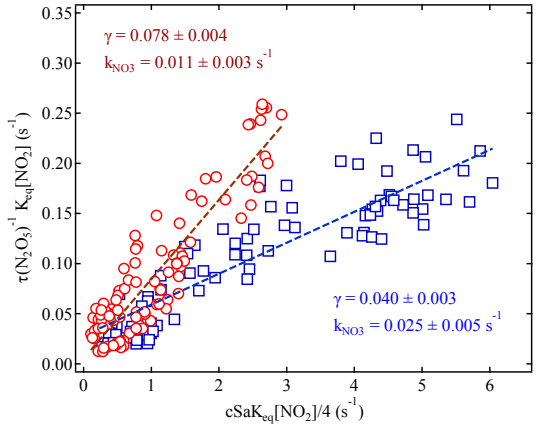

Figure 7. Example fits of inverse N_2O_5 steady-state lifetimes according to Eq. (5) for two cases observed on the nights of 2 and 21 August 2014. The best fit values of γ and k_{NO_3} are shown.

significantly higher than those determined from a mountain site in southern China (Brown et al., 2016) and from tower and aircraft measurements in the USA (e.g., Brown et al., 2009; Wagner et al., 2013).

The NO_3 reactivity, or loss rate coefficient $k(NO_3)$, can be estimated from the sum of the products of measured VOC concentrations and the bimolecular rate coefficients for the corresponding NO_3–VOC reactions (Atkinson and Arey, 2003):

$$k\,(\mathrm{NO_3}) = k_{\mathrm{NO+NO_3}}[\mathrm{NO}] + \sum_i k_i\,[\mathrm{VOC}_i]\,. \quad (4)$$

Because of the lack of concurrent VOC measurements in the present study, we used the average VOC speciations measured before sunrise and in the evening at Mt. Tai during our previous study in 2007 (cf. Table S1 in the Supplement) to estimate $k(NO_3)$. The determined nighttime $k(NO_3)$ was $1.33 \times 10^{-2}\,s^{-1}$ for the first half of the night and $1.07 \times 10^{-2}\,s^{-1}$ for the period after midnight, which is equivalent to an NO_3 lifetime of approximately 1.5 min. The estimated $k(NO_3)$ could be considered as an upper limit for coal-fired plumes because of potential lower biogenic VOC levels within the plumes. The estimation here does not account for the VOC changes between years and the night to night variability, which may result in uncertainties. The $k(NO_3)$ derived by another approach, i.e., from the nighttime steady-state fits, provides a consistency check and evaluation of the errors, as described below.

The heterogeneous loss rate, $k(N_2O_5)_{het}$, can be obtained by subtracting the $k(NO_3)/K_{eq}[NO_2]$ from the determined $\tau(N_2O_5)^{-1}$ in Eq. (3). Figure 6a shows the averaged total N_2O_5 reactivity and fractions of N_2O_5 loss via NO_3 ($k(NO_3)/K_{eq}[NO_2]$) and heterogeneous N_2O_5 loss during the study period. As shown, the heterogeneous loss was dominant, accounting for 70–80 % of total N_2O_5 reactivity, with a higher fraction before midnight. Figure 6b shows the contribution of different VOC categories to the average first-order NO_3 loss rate coefficients, $k(NO_3)$. Biogenic monoterpenes accounted for more than half of the NO_3 reactivity, followed by anthropogenic alkenes (such as butene), isoprene, and dimethyl sulfide (DMS). Aromatics and alkanes made small contributions (< 1 %) to the total NO_3 reactivity. Although some unmeasured organic species (e.g., peroxy radicals) could also contribute to a small fraction of NO_3 loss (Brown et al., 2011; Edwards et al., 2017), the dominant NO_3 reactivity by biogenic VOCs is similar to that observed at a mountain site in southern China (Brown et al., 2016) and in aircraft measurement in residual layer in the southeast USA (Edwards et al., 2017), whereas the anthropogenic contribution is much higher in the present study. The estimated NO_3 activity is slightly lower than that obtained from surface site measurements in the NCP (Tham et al., 2016; X. Wang et al., 2017), which is in line with the higher abundances of VOCs in the polluted boundary layer.

3.3.2 N_2O_5 uptake coefficient

Because the N_2O_5 uptake coefficient γ is related to the first-order loss rate coefficient of N_2O_5, $k(N_2O_5)_{het}$ (Eq. 1), then Eq. (3) can be expressed as follows:

$$\tau\,(\mathrm{N_2O_5})^{-1} K_{\mathrm{eq}}\,[\mathrm{NO_2}] \approx k\,(\mathrm{NO_3}) + \frac{1}{4} c_{\mathrm{N_2O_5}} S_{\mathrm{a}} K_{\mathrm{eq}}\,[\mathrm{NO_2}]\,\gamma_{\mathrm{N_2O_5}}\,. \quad (5)$$

The linear relationship between the left-hand side of Eq. (5) and $1/4 c_{N_2O_5} S_a K_{eq}[NO_2]$ will give the N_2O_5 uptake coefficient γ as the slope and the NO_3 loss rate coefficient $k(NO_3)$ as the intercept (Brown et al., 2009). We selected data for periods in which $d[N_2O_5]/dt$ is close to zero and the lifetime is relatively stable, which best corresponds to steady-state conditions. Figure 7 shows two examples of $\tau(N_2O_5)^{-1} K_{eq}[NO_2]$ vs. $1/4 c_{N_2O_5} S_a K_{eq}[NO_2]$ for cases observed on the nights of 2 and 21 August 2014. The γ and $k(NO_3)$ values derived from the linear fits are $\gamma = 0.040$ and

Table 2. Statistical summary of determined N_2O_5 uptake coefficients γ, $ClNO_2$ yields ϕ, nitrate formation rates, and nocturnal NO_x removal rates at Mt. Tai during the study period.

	$\gamma_{N_2O_5}$	k_{NO_3}	ϕ_{ClNO_2}	NO_3^- formation rate (pptv s^{-1})	NO_3^- formation rate ($\mu g\,m^{-3}\,h^{-1}$)	NO_x removal rate (ppbv h^{-1})	NO_x loss rate coefficient (h^{-1})
Mean	0.061	0.015	0.28	0.29	2.2	1.12	0.24
SD	0.025	0.010	0.24	0.18	1.4	0.63	0.08
Median	0.070	0.011	0.20	0.26	2.0	0.98	0.24
Min	0.021	0.003	0.02	0.02	0.2	0.19	0.05
Max	0.102	0.034	0.90	0.62	4.8	2.34	0.38

$k(NO_3) = 0.025\,s^{-1}$ for the 2 August case and $\gamma = 0.078$ and $k(NO_3) = 0.011\,s^{-1}$ for the 21 August case. Similar analyses were performed for 11 additional cases during the campaign, and the derived results are summarized in Table 2. The determined γ values range from 0.021 to 0.102, with a mean value of 0.061 ± 0.025. The average $k(NO_3)$ derived from the steady-state fits is $0.015 \pm 0.010\,s^{-1}$, which is comparable to that predicted from the VOC concentrations described above, indicating that the estimated results in the present study are reliable and likely representative of averaged conditions in the region. The agreement between these two methods also corroborates the determination of the uptake coefficient from steady-state analysis. The estimated uncertainty in each individual determination varied from 35 to 100 %, including statistical errors and uncertainty associated with measurements of gaseous and aerosol species (Tham et al., 2016).

Compared with the previous field-determined N_2O_5 uptake coefficients (0.002–0.04) from aircraft, tower, and mountaintop measurements in the USA and southern China (e.g., Brown et al., 2006, 2016; Morgan et al., 2015), the observed γ values in the present study are significantly higher. The large variability of γ at Mt. Tai is similar to that observed at a rural high-elevation site in Germany and a tower measurement in Colorado, with γ ranging from 10^{-3} to 0.11 (Wagner et al., 2013; Phillips et al., 2016). The overall higher averaged γ value at Mt. Tai is likely associated with the high RH and aerosol composition with high sulfate but low organic fractions, the condition of which favors more efficient N_2O_5 uptake (Brown et al., 2006; Wagner et al., 2013; Phillips et al., 2016). A recent laboratory study has reported high γ (> 0.05) of isotope-labeled N_2O_5 into aqueous nitrate-containing aerosols and largely enhancement of uptake at higher RH conditions (Gržinić et al., 2017), which help rationalize our field results with a larger uptake coefficient than many previous studies. Moreover, a measurement at an urban surface site in Jinan close to Mt. Tai gave similarly high values of γ (0.042–0.092) (X. Wang et al., 2017). This may suggest a unique feature of the reactive nitrogen chemistry, with rapid heterogeneous N_2O_5 loss over this region, and is consistent with the observed low N_2O_5 levels but relatively high $ClNO_2$ and particulate nitrate produced from the heterogeneous reactions.

Previous laboratory studies have investigated the dependence of γ on aerosol compositions and have developed mechanistic parameterizations of γ that can be employed in air quality models (Chang et al., 2011, and references therein). A commonly used parameterization was proposed by Bertram and Thornton (2009) and considered the aerosol volume-to-surface ratio (V/S), concentrations of nitrate, chloride, and water. For comparison, γ values were calculated using this parameterization based on the measured aerosol composition and molarity of water determined from the thermodynamic model with inputs of NH_4^+, Na^+, SO_4^{2-}, NO_3^-, and Cl^- (E-AIM model IV, http://www.aim.env.uea.ac.uk/aim/model4/model4a.php) (Wexler and Clegg, 2002). An error estimation showed that a 3 % change in RH implies an uncertainty in the particle liquid water content of ~ 5 %. In the calculation, mean values of V/S (64.8 - 77.2 nm) measured in the present study instead of empirical prefactor A were used, and the reaction rate coefficients were employed as the empirical values suggested by Bertram and Thornton (2009).

Figure 8 shows a comparison of the γ values (with total uncertainty) determined from parameterization and measurements. Overall, the parameterized γ shows good correlation ($r = 0.87$) with the observation-determined values and gives an average of 0.063 ± 0.006, which is in good agreement with the average of 0.061 ± 0.025 derived from steady-state analysis. However, the γ values from the parameterization are in the range of 0.052–0.070, with much lower variability than the measurement-determined values. Similar results with compatible averaged γ values between measurements and parameterization predictions but higher variability for measurement-derived γ have been reported at a mountain measurement in Germany (Phillips et al., 2016). A distinct difference of γ between the steady-state analysis and the parameterization has also been reported by Chang et al. (2016), who suggested that the uncertainty in determining aerosol water content would introduce errors in the parameterization. Bertram and Thornton (2009) suggested that predicted γ val-

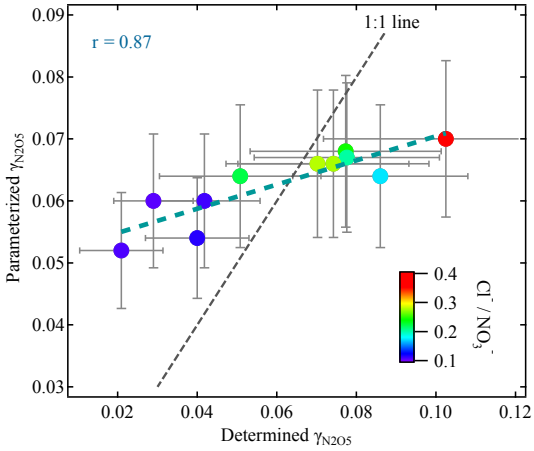

Figure 8. Comparison of field-determined γ with that derived from the parameterization of Bertram and Thornton (2009). The colors of the markers indicate the corresponding concentration ratio of particulate chloride to nitrate. The error bars represent the total aggregate uncertainty associated with measurement and derivation.

ues would plateau and be independent of particulate chemical composition at particle water molarity above 15 M. In the present study, the particle water molarity in these cases was consistently above 25 M because of the high RH and frequent cloud cover at the mountain site, which may explain the lower variability of γ values predicted by parameterization.

A moderate negative dependence ($r = 0.54$) of determined γ on aerosol nitrate concentration can be inferred, with lower values of γ associated with higher nitrate content (cf. Fig. S2a). This pattern is consistent with the nitrate suppress effect on N_2O_5 uptake identified in previous laboratory studies (Mentel et al., 1999) and is also similar to the anti-correlation of γ and nitrate from tower measurements in the USA and aircraft measurements over the UK (Wagner et al., 2013; Morgan et al., 2015). The relationship between the γ with the aerosol water to nitrate ratio also exhibits a consistent trend with the previous observations and parameterizations (e.g., Bertram and Thornton, 2009; Morgan et al., 2015), with increasing uptake as the ratio increases (Fig. S2b).

Furthermore, as suggested by Bertram and Thornton (2009), the presence of chloride can offset the suppression of N_2O_5 uptake by nitrate. The determined γ values in the present study also show positive dependence on aerosol chloride concentration ($r = 0.59$), indicating the enhancement of N_2O_5 uptake by increased chloride contents in aerosols. This can be better described by the clear positive dependence ($r = 0.84$) of γ on the molar ratio of particulate chloride to nitrate, as illustrated by the color-coded data in Figs. 8 and S3b. The variation in γ values determined in the present study appears to be controlled largely by the particulate chloride-to-nitrate ratio, broadly following the competing effects of nitrate and chloride in the parameterization (Bertram and Thornton, 2009; Ryder et al., 2014). However, the discrepancy between the measurement- and parameterization-derived values may imply that some mechanisms and factors affecting γ under conditions of high humid and pollution (e.g., reacto-diffusive length, salting effects) (Gaston and Thornton, 2016; Gržinić et al., 2017) should be further explicitly considered in the parameterization. The in situ $\gamma_{N_2O_5}$ measurement technique developed by Bertram et al. (2009a) may be useful in directly investigating the complex dependence of γ on different factors in a range of environments.

3.4 $ClNO_2$ production yield

To characterize the formation of $ClNO_2$ from rapid heterogeneous N_2O_5 uptake and sufficient particulate chloride, the yields of $ClNO_2$ (ϕ) were examined for different plumes. For regional diffuse pollution cases, the ϕ defined in Reaction (R3) can be estimated from the ratio between $ClNO_2$ production rate and N_2O_5 loss rate, as the first term in below equation.

$$\Phi = \frac{\mathrm{d}ClNO_2/\mathrm{d}t}{k(N_2O_5)_{het}[N_2O_5]} = \frac{[ClNO_2]}{\int k(N_2O_5)_{het}[N_2O_5]\,\mathrm{d}t} \quad (6)$$

$k(N_2O_5)$ values can be determined using the inverse steady-state lifetime analysis described above in Eq. (3), and the production rate of $ClNO_2$ can be derived from the near-linear increase in $ClNO_2$ mixing ratio observed during a period when the related species (e.g., NO_x, SO_2) and environmental variables (e.g., temperature, RH) were roughly constant. The approach here assumes that the relevant properties of the nocturnal air mass are conserved and neglects other possible sources and sinks of $ClNO_2$ in the air mass history. For the intercepted coal-fired plumes exhibiting sharp $ClNO_2$ peaks, the $ClNO_2$ yield can be estimated from the ratio of the observed $ClNO_2$ mixing ratio to the integrated N_2O_5 uptake loss over the plume age (i.e., the second term in Eq. 6). The analysis assumes that no $ClNO_2$ was present at the point of plume emission from the combustion sources and no $ClNO_2$ formation before sunset, and that the γ and ϕ within the plumes did not change during the transport from the source to the measurement site. The potential variability in these quantities likely bias the estimates, but these assumptions are a necessary simplification to represent the averaged values that best describe the observations. It should be noted that the steady-state N_2O_5 loss rate is crucial in the yield estimation, which could be underestimated by potentially overestimating the loss rate in some cases with large uncertainties in N_2O_5 measurement and NO_3 reactivity analysis. Therefore, an alternative approach suggested by Riedel et al. (2013) was also applied to derive the $ClNO_2$ yield from the ratio of enhancements of $ClNO_2$ and total nitrate (aerosol $NO_3^- + HNO_3$) in the cases. Given the low time resolution of nitrate data that could potentially introduce large uncertainties, this approach

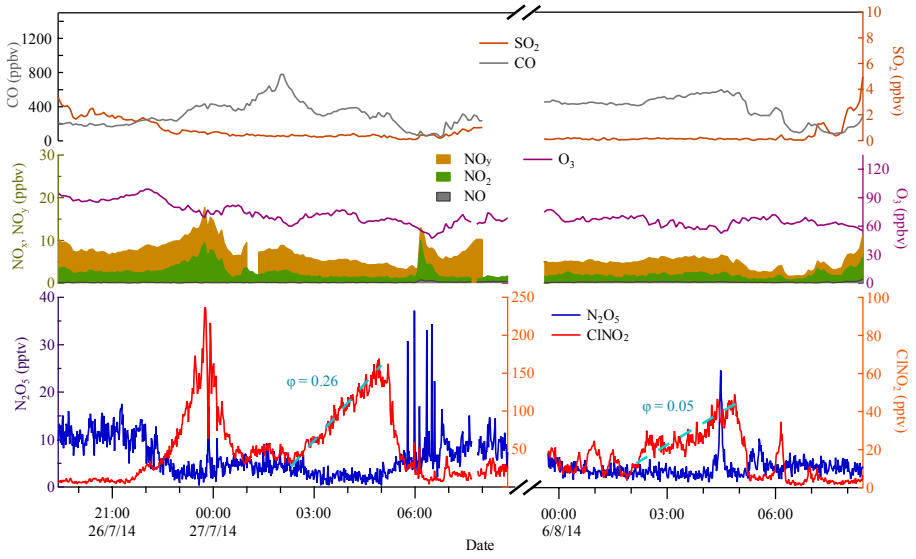

Figure 9. Examples of $ClNO_2$ yields determined for two cases on 27 July and 6 August 2014. The $ClNO_2$ mixing ratios increased steadily, while those of NO_x, O_3, and SO_2 did not change significantly during the studied periods.

will only be used as a reference to validate the former analysis based on Eq. (6).

Two examples of the yield analysis are shown in Fig. 9, which indicate the time periods in which $ClNO_2$ concentration increased while other parameters (such as N_2O_5, NO_x, O_3, and SO_2 concentrations) were relatively stable. The ϕ values obtained for these two cases were 0.26 and 0.05 for 27 July and 6 August, respectively. Similar analyses were performed for all of other selected cases in which the $ClNO_2$ concentration increased and other relevant parameters were relatively constant for a short period, typically 2–3 h, and the obtained results were summarized in Table 2. The determined ϕ for the seven coal-fired plumes are also listed in Table 1. During the measurement period, ϕ varied from 0.02 to 0.90, with an average of 0.28 ± 0.24 and a median of 0.22. In comparison, the ϕ derived from the production ratio approach showed comparable results with an average of 0.25 ± 0.17, and the ϕ values from two different approaches match reasonably well with a reduced major axis regression (RMA) slope of 0.78 ± 0.08 and r^2 of 0.73 (cf. Fig. S4), which corroborates the yield analysis and indicates that the differences are within the overall uncertainty of 40 %. The large variability of ϕ is similar to field-derived values in most previous studies, and the mean value is comparable to that in the nocturnal residual layer over continental Colorado (0.18) (Thornton et al., 2010), but lower than that observed at a mountain site in Germany (0.49) (Phillips et al., 2016). The ϕ values for the coal-fired plumes (range of 0.20–0.90; average of 0.46 ± 0.24) are generally higher than the campaign average and those from regional diffuse pollution cases. The maximum ϕ (0.90) corresponds to the plume with the highest $ClNO_2$ mixing ratio observed during the campaign. This is consistent with a tower measurement in Colorado, in which higher $ClNO_2$ yields were also observed in inland power plant plumes (Riedel et al., 2013). Similar to that developed for γ, a parameterization of $ClNO_2$ yield as a function of aerosol water and chlorine composition has been proposed based on laboratory studies (Bertram and Thornton, 2009; Roberts et al., 2009):

$$\Phi = \frac{[Cl^-]}{k'[H_2O] + [Cl^-]}. \quad (7)$$

We compared the field-derived values to the parameterization for cases with available aerosol compositions, using an empirical k' of 1/450, as recommended by Roberts et al. (2009). The particle liquid water content $[H_2O]$ was calculated from the thermodynamic model (E-AIM model IV) based on measured aerosols composition, as described above. As shown in Fig. 10a, the ϕ values predicted by the parameterization are generally higher than those determined from observed $ClNO_2$ production rates, especially at low measurement-determined yields. For measured ϕ values higher than 0.4, smaller differences (< 20 %) were observed between the two methods, which are within the aggregate uncertainty associated with measurement and derivation. The parameterized ϕ values exhibit positive dependence on the aerosol chloride concentration and the Cl^-/H_2O ratio, as shown by the color code in Fig. 10a. The measurement-determined values only exhibit such measurable dependence at low yields, implying the possible biased relationship due to higher aerosol water conditions in the present work. The discrepancy between the parameterization ϕ based upon aerosol composition and those derived from measured $ClNO_2$ concentrations has been found previously (e.g., Wagner et al., 2013), and the underlying causes have not been resolved.

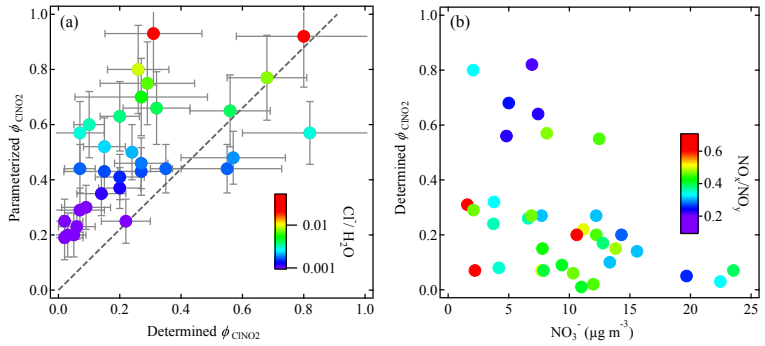

Figure 10. (a) Comparison of field-determined ϕ with that derived from parameterization (Eq. 7) – the colors of the markers represent the corresponding Cl^-/H_2O ratio; **(b)** relationship between field-determined ϕ and measured nitrate concentrations in aerosols – the colors of markers represent the corresponding NO_x/NO_y ratio. The error bars represent the total aggregate uncertainty similar to Fig. 8.

By examining the relationships between the determined yield and other parameters, we found a slightly negative relationship between ϕ and particulate nitrate concentration, as depicted in Fig. 10b. Although the data are scattered, the high-yield cases are mostly associated with lower nitrate concentrations, while the ϕ values for the high nitrate cases ($> 15\,\mu g\,m^{-3}$) are smaller. A similar trend was observed for the NO_x/NO_y ratio, which indicates the "age" of the air masses, suggesting that higher ϕ values are usually associated with relatively "young" air masses exhibiting low nitrate concentrations. More secondary and dissolved organic matters in aged aerosols could be a possible factor contributing to the reduction of $ClNO_2$ production efficiency (Mielke et al., 2013; Ryder et al., 2015; Phillips et al., 2016). Further studies are needed to characterize the combined effects of various parameters on $ClNO_2$ yields, in particular the influences of the aerosol mixing state, chloride availability distribution among particle sizes, organic matter, acidity, other possible loss ways of $ClNO_2$, and potential factors affecting in high humid and polluted conditions (Laskin et al., 2012; Mielke et al., 2013; Wagner et al., 2013; Ryder et al., 2015; Li et al., 2016; Phillips et al., 2016).

3.5 Effects of heterogeneous N_2O_5 reactions on nitrate formation and NO_x processing

In addition to abundant $ClNO_2$ formation, rapid heterogeneous N_2O_5 uptake may also lead to the production of a large amount of nitrate, which is one of the main components of fine particles contributing to haze pollution in northern China (e.g., Huang et al., 2014). Based on the reactions described above, the formation rate of soluble nitrate from N_2O_5 reactions, $p(NO_3^-)$, can be determined from the $ClNO_2$ yield and N_2O_5 heterogeneous loss rate as follows:

$$p\left(NO_3^-\right) = (2-\phi)k_{N_2O_5}[N_2O_5]. \quad (8)$$

The $p(NO_3^-)$ values obtained for the select cases during the study period ranged from 0.02 to 0.62 pptv s^{-1}, with a mean value of 0.29 ± 0.18 pptv s^{-1}, corresponding to 0.2–4.8 μg m^{-3} h^{-1} and 2.2 ± 1.4 μg m^{-3} h^{-1} (Table 2). The derived rates are comparable to the observed increases in nitrate concentrations (2–5 μg m^{-3} h^{-1}) during haze episodes in summer nights at a rural site in the NCP (Wen et al., 2015). By assuming that produced nitrate is conserved and neglecting the deposition and volatilization loss (e.g., via ammonium nitrate), the in situ NO_3^- formation could be predicted by integrating each derived formation rate over the corresponding analysis period. Similar to the N_2O_5 uptake coefficient and $ClNO_2$ yield determination above, the nitrate formation estimation here assumes a conserved air mass with a constant formation rate over the study period. For coal-fired plumes, we equated the measured nitrate concentrations with the increases by assuming that no aerosol nitrate was directly emitted from the nocturnal point sources. As shown in Fig. 11, the predicted nitrate formation shows reasonable agreement with the measured increases in nitrate concentrations (ΔNO_3^-) (RMA slope of 1.14 and r of 0.81). This consistency also can serve as a check to validate the reliability of the above-determined heterogeneous N_2O_5 reactivity and parameters of γ and ϕ. The in situ nitrate formation from heterogeneous N_2O_5 reactions was predicted to be as high as 17 μg m^{-3}, with a mean value of 4.3 ± 4.5 μg m^{-3}, accounting for 32 (±27) % of the observed average nitrate concentration during the cases. This is consistent with the maximum nitrate increase of 14.9 μg m^{-3} over south China (Li et al., 2016) and the 21 % nitrate increase in polluted episodes in Beijing (Su et al., 2017) after considering the heterogeneous N_2O_5 uptake in the regional model simulation. As for a plume undergoing continuous chemical processing from dusk to sunrise, the heterogeneous N_2O_5 reactions would lead to substantial nitrate formation (e.g., 22 μg m^{-3} production for a 10 h night) and could contribute significantly to secondary fine aerosols as the main driver of the persistent haze pollution in northern China.

The formation of nitrate (including HNO_3) and its subsequent removal by deposition is the predominant removal

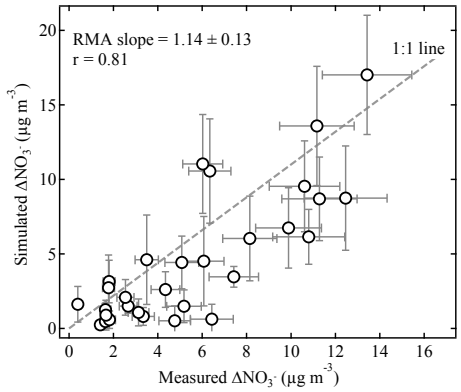

Figure 11. Comparison of predicted nitrate production based on integrating the derived nitrate formation rate with the measured increase in nitrate concentrations (ΔNO_3^-) over the analysis time period.

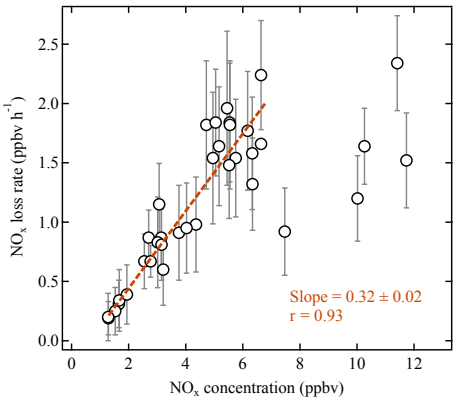

Figure 12. Relationship between determined NO_x loss rate and observed ambient NO_x concentration at the measurement site during the study period.

mechanism of nitrogen oxides from the atmosphere (Chang et al., 2011). The nocturnal NO_x removal rate depends on the NO_3 radical production rate, heterogeneous N_2O_5 loss rate, NO_3 reaction rate with VOCs, the partitioning between N_2O_5 and NO_3 concentrations, and $ClNO_2$ yield. $ClNO_2$ mainly functions as a reservoir of NO_x, rather than as a sink, because the formation of $ClNO_2$ throughout the night with subsequent morning photolysis recycles NO_2 (Behnke et al., 1997). The reactions of NO_3 with VOCs would predominantly produce organic nitrate products (Brown and Stutz, 2012, and references therein), but some fraction of NO_2 can be regenerated in the NO_3 reactions, i.e., with terpenes (e.g., Wängberg et al., 1997), or released from the decomposition of organic nitrate during the transport (e.g., Francisco and Krylowski, 2005). For simplicity, we neglect the recycling of NO_2 from NO_3–VOC reactions by assuming the complete removal of reactive nitrogen (Wagner et al., 2013). This would overestimate the NO_x loss since the monoterpenes contribute to around half of NO_3 reactivity in the present study, but this assumption does not significantly affect the conclusion because the NO_3 loss with VOCs was the minor path compared to N_2O_5 heterogeneous loss. Thus, the nocturnal NO_x loss rate can be quantified by the following equation:

$$L(NO_x) = (2-\phi)k_{N_2O_5}[N_2O_5] + k_{NO_3}[NO_3] = (1-\phi)k_{N_2O_5}[N_2O_5] + p[NO_3]. \quad (9)$$

Using the coefficients described above, we calculated the nocturnal loss rate of NO_x for each case, as summarized in Table 2. The NO_x removal rate varied from 0.19 to 2.34 ppbv h^{-1}, with a mean of 1.12 ± 0.63 ppbv h^{-1}, which corresponds to a pseudo-first-order loss rate coefficient of $0.24 \pm 0.08\,h^{-1}$ on average for the studied cases. This loss rate is higher than that determined from a mountain site measurement in Taunus, Germany (~ 0.2 ppbv h^{-1} with typical NO_2 level of 1–2 ppbv) (Crowley et al., 2010), and the results from aircraft measurements in the USA over Ohio, Pennsylvania, and the downwind region of New York (90 and 50 % NO_x loss in a 10 h night, respectively) (Brown et al., 2006). For reference, this nocturnal average loss rate is approximately equivalent to NO_2 loss via reaction with OH in afternoon condition assuming an OH concentration of around 2×10^6 molecules cm^{-3}, indicating the importance of nocturnal heterogeneous reactions on NO_x processing and budget. Figure 12 shows the relationship between determined NO_x loss rate and observed ambient NO_x concentration at the measurement site. NO_x loss rate appears to be strongly dependent upon NO_x concentrations below 6 ppbv (slope $= 0.32\,h^{-1}$; $r = 0.93$); the loss rate became more scattered at higher NO_x conditions, which were typically observed in the coal-fired power plant and industrial plumes. This result implies that for low-NO_x conditions (< 6 ppbv), 96 % of NO_x would be removed after 3 h of nocturnal processing, if no additional NO_x emissions affect the plume during this period.

Comparing NO_x loss to the nitrate formation rates, it can be inferred that the nitrate formation from heterogeneous N_2O_5 uptake is predominant in reactive NO_x loss and accounts for an average of 87 % of the NO_x loss, although this fraction of individual cases varied between 35 and 100 %. A box model simulation based on tower measurements at Colorado also reported that the largest proportion of the nitrate radical chemistry is N_2O_5 hydrolysis, which typically accounted for 80 % of nitrate radical production, whereas the losses to NO_3–VOC reactions are less than 10 % (Wagner et al., 2013). A recent model simulation for southern China also suggested that considering the N_2O_5 uptake and subsequent Cl activation could decrease regional NO_x by more than 16 % (Li et al., 2016). The results obtained in the present study demonstrate the significance of fast heterogeneous N_2O_5 chemistry on nocturnal NO_x removal and fine nitrate formation in the polluted residual layer over the NCP.

4 Summary and conclusions

An intensive field study was conducted at a high-altitude site to characterize the reactive nitrogen chemistry in the polluted nocturnal residual layer over the NCP. The results revealed the frequently elevated $ClNO_2$ mixing ratios (maximum of 2065 pptv) and efficient $ClNO_2$ yields (0.46 ± 0.24) resulting from power plant and industrial plumes in the residual layer. The presence of $ClNO_2$-laden air in the nocturnal residual layer confirms our previous hypothesis, based on a measurement in a rural site in the NCP, that the downward mixing of $ClNO_2$-rich air into the surface in the next morning would have large impacts on early morning photochemistry and ozone production. Rapid heterogeneous N_2O_5 uptake and efficient $ClNO_2$ and nitrate formation were observed during the study period. The γ values determined in the present study (average of 0.061 ± 0.025) exhibited a clear dependence on the particulate chloride-to-nitrate ratio and are higher than those observed in other locations, but consistent with those obtained at a surface site in the same region of the NCP. Laboratory-derived parameterizations predicted comparable mean γ values, but did not represent the high variability of the measured values, and tended to overestimate ϕ in the low yields. These discrepancies suggest that various aerosol physicochemical parameters have complicated effects on N_2O_5 uptake and $ClNO_2$ yield, in particular in a high-humidity and polluted residual layer, which requires further investigation.

Fast heterogeneous N_2O_5 uptake dominated and accounted for a mean of 87 % of the regional nocturnal NO_x loss during the study periods in the NCP. The estimated nocturnal loss rate of NO_x is higher than that previously observed in the USA and Europe, with an averaged loss rate and rate coefficient of 1.12 ± 0.63 ppbv h^{-1} and $0.24 \pm 0.08\,h^{-1}$, respectively. Moreover, heterogeneous reactions contributed to substantial nitrate production of up to 17 µg m^{-3}, with a mean nocturnal formation rate of 2.2 ± 1.4 µg m^{-3} h^{-1}, and in situ production could account for 32 ± 27 % of the observed nitrate concentrations in the studied cases. The results may help explain the previously observed rapid nighttime growth of fine nitrate aerosols in the NCP and demonstrate the importance of heterogeneous N_2O_5–$ClNO_2$ chemistry on NO_x and aerosol budgets in the polluted residual layer over the NCP, which underpins the need for further studies regarding their roles in the formation of complex haze pollution in northern China.

Data availability. The data used in this study are available upon request from the corresponding author (z.wang@polyu.edu.hk).

The Supplement related to this article is available online at https://doi.org/10.5194/acp-17-12361-2017-supplement.

Competing interests. The authors declare that they have no conflict of interest.

Special issue statement. This article is part of the special issue "Regional transport and transformation of air pollution in eastern China". It is not associated with a conference.

Acknowledgements. The authors would like to thank Fu Xiao for help in providing the location information of power plants in Shandong. The HYSPLIT model was made available by the NOAA Air Resources Laboratory. This work was funded by the National Natural Science Foundation of China (91544213, 41505103, 41275123), PolyU Project of Strategic Importance (1-ZE13), and the National Key R & D Program of China (No. 2016YFC0200503). The authors also acknowledge the support of the Research Institute for Sustainable Urban Development (RISUD).

Edited by: David Parrish
Reviewed by: three anonymous referees

References

Abbatt, J., Lee, A., and Thornton, J.: Quantifying trace gas uptake to tropospheric aerosol: recent advances and remaining challenges, Chem. Soc. Rev., 41, 6555–6581, 2012.

Ammann, M., Cox, R. A., Crowley, J. N., Jenkin, M. E., Mellouki, A., Rossi, M. J., Troe, J., and Wallington, T. J.: Evaluated kinetic and photochemical data for atmospheric chemistry: Volume VI – heterogeneous reactions with liquid substrates, Atmos. Chem. Phys., 13, 8045–8228, https://doi.org/10.5194/acp-13-8045-2013, 2013.

Anttila, T., Kiendler-Scharr, A., Tillmann, R., and Mentel, T. F.: On the Reactive Uptake of Gaseous Compounds by Organic-Coated Aqueous Aerosols: Theoretical Analysis and Application to the Heterogeneous Hydrolysis of N_2O_5, J. Phys. Chem. A, 110, 10435–10443, 2006.

Atkinson, R. and Arey, J.: Atmospheric Degradation of Volatile Organic Compounds, Chem. Rev., 103, 4605–4638, 2003.

Behnke, W., George, C., Scheer, V., and Zetzsch, C.: Production and decay of $ClNO_2$ from the reaction of gaseous N_2O_5 with NaCl solution: Bulk and aerosol experiments, J. Geophys. Res.-Atmos., 102, 3795–3804, https://doi.org/10.1029/96jd03057, 1997.

Bertram, T. H. and Thornton, J. A.: Toward a general parameterization of N_2O_5 reactivity on aqueous particles: the competing effects of particle liquid water, nitrate and chloride, Atmos. Chem. Phys., 9, 8351–8363, https://doi.org/10.5194/acp-9-8351-2009, 2009.

Bertram, T. H., Thornton, J. A., and Riedel, T. P.: An experimental technique for the direct measurement of N_2O_5 reactivity on ambient particles, Atmos. Meas. Tech., 2, 231–242, https://doi.org/10.5194/amt-2-231-2009, 2009a.

Bertram, T. H., Thornton, J. A., Riedel, T. P., Middlebrook, A. M., Bahreini, R., Bates, T. S., Quinn, P. K., and Coffman, D. J.: Direct observations of N_2O_5 reactivity on am-

bient aerosol particles, Geophys. Res. Lett., 36, L19803, https://doi.org/10.1029/2009GL040248, 2009b.

Brown, S. S. and Stutz, J.: Nighttime radical observations and chemistry, Chem. Soc. Rev., 41, 6405–6447, https://doi.org/10.1039/C2CS35181A, 2012.

Brown, S. S., Osthoff, H. D., Stark, H., Dubé, W. P., Ryerson, T. B., Warneke, C., de Gouw, J. A., Wollny, A. G., Parrish, D. D., and Fehsenfeld, F. C.: Aircraft observations of daytime NO_3 and N_2O_5 and their implications for tropospheric chemistry, J. Photochem. Photobiol. A, 176, 270–278, 2005.

Brown, S. S., Ryerson, T., Wollny, A., Brock, C., Peltier, R., Sullivan, A., Weber, R., Dube, W., Trainer, M., and Meagher, J.: Variability in nocturnal nitrogen oxide processing and its role in regional air quality, Science, 311, 67–70, 2006.

Brown, S. S., Dubé, W. P., Osthoff, H. D., Stutz, J., Ryerson, T. B., Wollny, A. G., Brock, C. A., Warneke, C., de Gouw, J. A., Atlas, E., Neuman, J. A., Holloway, J. S., Lerner, B. M., Williams, E. J., Kuster, W. C., Goldan, P. D., Angevine, W. M., Trainer, M., Fehsenfeld, F. C., and Ravishankara, A. R.: Vertical profiles in NO_3 and N_2O_5 measured from an aircraft: Results from the NOAA P-3 and surface platforms during the New England Air Quality Study 2004, J. Geophys. Res.-Atmos., 112, D22304, https://doi.org/10.1029/2007JD008883, 2007.

Brown, S. S., Dubé, W. P., Fuchs, H., Ryerson, T. B., Wollny, A. G., Brock, C. A., Bahreini, R., Middlebrook, A. M., Neuman, J. A., Atlas, E., Roberts, J. M., Osthoff, H. D., Trainer, M., Fehsenfeld, F. C., and Ravishankara, A. R.: Reactive uptake coefficients for N_2O_5 determined from aircraft measurements during the Second Texas Air Quality Study: Comparison to current model parameterizations, J. Geophys. Res.-Atmos., 114, D00F10, https://doi.org/10.1029/2008JD011679, 2009.

Brown, S. S., Dubé, W. P., Peischl, J., Ryerson, T. B., Atlas, E., Warneke, C., de Gouw, J. A., te Lintel Hekkert, S., Brock, C. A., Flocke, F., Trainer, M., Parrish, D. D., Feshenfeld, F. C., and Ravishankara, A. R.: Budgets for nocturnal VOC oxidation by nitrate radicals aloft during the 2006 Texas Air Quality Study, J. Geophys. Res.-Atmos., 116, D24305, https://doi.org/10.1029/2011JD016544, 2011.

Brown, S. S., Dubé, W. P., Tham, Y. J., Zha, Q., Xue, L., Poon, S., Wang, Z., Blake, D. R., Tsui, W., Parrish, D. D., and Wang, T.: Nighttime Chemistry at a High Altitude Site Above Hong Kong, J. Geophys. Res.-Atmos., 121, 2457–2475, https://doi.org/10.1002/2015jd024566, 2016.

Chang, W. L., Bhave, P. V., Brown, S. S., Riemer, N., Stutz, J., and Dabdub, D.: Heterogeneous Atmospheric Chemistry, Ambient Measurements, and Model Calculations of N_2O_5: A Review, Aerosol Sci. Tech., 45, 665–695, https://doi.org/10.1080/02786826.2010.551672, 2011.

Chang, W. L., Brown, S. S., Stutz, J., Middlebrook, A. M., Bahreini, R., Wagner, N. L., Dubé, W. P., Pollack, I. B., Ryerson, T. B., and Riemer, N.: Evaluating N_2O_5 heterogeneous hydrolysis parameterizations for CalNex 2010, J. Geophys. Res.-Atmos., 121, 5051–5070, https://doi.org/10.1002/2015JD024737, 2016.

Crowley, J. N., Schuster, G., Pouvesle, N., Parchatka, U., Fischer, H., Bonn, B., Bingemer, H., and Lelieveld, J.: Nocturnal nitrogen oxides at a rural mountain-site in south-western Germany, Atmos. Chem. Phys., 10, 2795–2812, https://doi.org/10.5194/acp-10-2795-2010, 2010.

Davis, J. M., Bhave, P. V., and Foley, K. M.: Parameterization of N_2O_5 reaction probabilities on the surface of particles containing ammonium, sulfate, and nitrate, Atmos. Chem. Phys., 8, 5295–5311, https://doi.org/10.5194/acp-8-5295-2008, 2008.

Draxler, R. R. and Hess, G. D.: An overview of the HYSPLIT_4 modelling system for trajectories, dispersion and deposition, Aust. Meteorol. Mag., 47, 295–308, 1998.

Edwards, P. M., Aikin, K. C., Dube, W. P., Fry, J. L., Gilman, J. B., de Gouw, J. A., Graus, M. G., Hanisco, T. F., Holloway, J., Hubler, G., Kaiser, J., Keutsch, F. N., Lerner, B. M., Neuman, J. A., Parrish, D. D., Peischl, J., Pollack, I. B., Ravishankara, A. R., Roberts, J. M., Ryerson, T. B., Trainer, M., Veres, P. R., Wolfe, G. M., Warneke, C., and Brown, S. S.: Transition from high- to low-NO_x control of night-time oxidation in the southeastern US, Nat. Geosci., 10, 490–495, https://doi.org/10.1038/ngeo2976, 2017.

Evans, M. J. and Jacob, D. J.: Impact of new laboratory studies of N_2O_5 hydrolysis on global model budgets of tropospheric nitrogen oxides, ozone, and OH, Geophys. Res. Lett., 32, L09813, https://doi.org/10.1029/2005GL022469, 2005.

Faxon, C., Bean, J., and Ruiz, L.: Inland Concentrations of Cl_2 and $ClNO_2$ in Southeast Texas Suggest Chlorine Chemistry Significantly Contributes to Atmospheric Reactivity, Atmosphere, 6, 1487, https://doi.org/10.3390/atmos6101487, 2015.

Finlayson-Pitts, B. J., Ezell, M. J., and Pitts, J. N.: Formation of chemically active chlorine compounds by reactions of atmospheric NaCl particles with gaseous N_2O_5 and $ClONO_2$, Nature, 337, 241–244, 1989.

Foley, K. M., Roselle, S. J., Appel, K. W., Bhave, P. V., Pleim, J. E., Otte, T. L., Mathur, R., Sarwar, G., Young, J. O., Gilliam, R. C., Nolte, C. G., Kelly, J. T., Gilliland, A. B., and Bash, J. O.: Incremental testing of the Community Multiscale Air Quality (CMAQ) modeling system version 4.7, Geosci. Model Dev., 3, 205–226, https://doi.org/10.5194/gmd-3-205-2010, 2010.

Francisco, M. A. and Krylowski, J.: Chemistry of Organic Nitrates: Thermal Chemistry of Linear and Branched Organic Nitrates, Indust. Eng. Chem. Res., 44, 5439–5446, https://doi.org/10.1021/ie049380d, 2005.

Gao, J., Wang, T., Ding, A., and Liu, C.: Observational study of ozone and carbon monoxide at the summit of mount Tai (1534 m a.s.l.) in central-eastern China, Atmos. Environ., 39, 4779–4791, 2005.

Gaston, C. J. and Thornton, J. A.: Reacto-Diffusive Length of N_2O_5 in Aqueous Sulfate- and Chloride-Containing Aerosol Particles, J. Phys. Chem. A, 120, 1039–1045, 2016.

Griffiths, P. T., Badger, C. L., Cox, R. A., Folkers, M., Henk, H. H., and Mentel, T. F.: Reactive Uptake of N_2O_5 by Aerosols Containing Dicarboxylic Acids. Effect of Particle Phase, Composition, and Nitrate Content, J. Phys. Chem. A, 113, 5082–5090, 2009.

Gržinić, G., Bartels-Rausch, T., Türler, A., and Ammann, M.: Efficient bulk mass accommodation and dissociation of N_2O_5 in neutral aqueous aerosol, Atmos. Chem. Phys., 17, 6493–6502, https://doi.org/10.5194/acp-17-6493-2017, 2017.

Guo, J., Wang, Y., Shen, X., Wang, Z., Lee, T., Wang, X., Li, P., Sun, M., Collett, J., Wang, W., and Wang, T.: Characterization of cloud water chemistry at Mount Tai, China: Seasonal variation, anthropogenic impact, and cloud processing, Atmos. Environ., 60, 467–476, https://doi.org/10.1016/j.atmosenv.2012.07.016, 2012.

Huang, R.-J., Zhang, Y., Bozzetti, C., Ho, K.-F., Cao, J.-J., Han, Y., Daellenbach, K. R., Slowik, J. G., Platt, S. M., Canonaco, F., Zotter, P., Wolf, R., Pieber, S. M., Bruns, E. A., Crippa, M., Ciarelli, G., Piazzalunga, A., Schwikowski, M., Abbaszade, G., Schnelle-Kreis, J., Zimmermann, R., An, Z., Szidat, S., Baltensperger, U., Haddad, I. E., and Prevot, A. S. H.: High secondary aerosol contribution to particulate pollution during haze events in China, Nature, 514, 218–222, 2014.

Laskin, A., Moffet, R. C., Gilles, M. K., Fast, J. D., Zaveri, R. A., Wang, B., Nigge, P., and Shutthanandan, J.: Tropospheric chemistry of internally mixed sea salt and organic particles: Surprising reactivity of NaCl with weak organic acids, J. Geophys. Res.-Atmos., 117, D15302, https://doi.org/10.1029/2012JD017743, 2012.

Li, Q., Zhang, L., Wang, T., Tham, Y. J., Ahmadov, R., Xue, L., Zhang, Q., and Zheng, J.: Impacts of heterogeneous uptake of dinitrogen pentoxide and chlorine activation on ozone and reactive nitrogen partitioning: improvement and application of the WRF-Chem model in southern China, Atmos. Chem. Phys., 16, 14875–14890, https://doi.org/10.5194/acp-16-14875-2016, 2016.

Liu, B. Y. H., Romay, F. J., Dick, W. D., Woo, K.-S., and Chiruta, M.: A Wide-Range Particle Spectrometer for Aerosol Measurement from 0.010 µm to 10 µm, Aerosol Air Qual. Res., 10, 125–139, https://doi.org/10.4209/aaqr.2009.10.0062, 2010.

Ma, N., Zhao, C., Tao, J., Wu, Z., Kecorius, S., Wang, Z., Größ, J., Liu, H., Bian, Y., Kuang, Y., Teich, M., Spindler, G., Müller, K., van Pinxteren, D., Herrmann, H., Hu, M., and Wiedensohler, A.: Variation of CCN activity during new particle formation events in the North China Plain, Atmos. Chem. Phys., 16, 8593–8607, https://doi.org/10.5194/acp-16-8593-2016, 2016.

Mentel, T. F., Sohn, M., and Wahner, A.: Nitrate effect in the heterogeneous hydrolysis of dinitrogen pentoxide on aqueous aerosols, Phys. Chem. Chem. Phys., 1, 5451–5457, https://doi.org/10.1039/A905338G, 1999.

Mielke, L. H., Furgeson, A., and Osthoff, H. D.: Observation of $ClNO_2$ in a Mid-Continental Urban Environment, Environ. Sci. Technol., 45, 8889–8896, 2011.

Mielke, L. H., Stutz, J., Tsai, C., Hurlock, S. C., Roberts, J. M., Veres, P. R., Froyd, K. D., Hayes, P. L., Cubison, M. J., Jimenez, J. L., Washenfelder, R. A., Young, C. J., Gilman, J. B., de Gouw, J. A., Flynn, J. H., Grossberg, N., Lefer, B. L., Liu, J., Weber, R. J., and Osthoff, H. D.: Heterogeneous formation of nitryl chloride and its role as a nocturnal NO_x reservoir species during CalNex-LA 2010, J. Geophys. Res.-Atmos., 118, 10638–10652, 2013.

Mielke, L. H., Furgeson, A., Odame-Ankrah, C. A., and Osthoff, H. D.: Ubiquity of $ClNO_2$ in the urban boundary layer of Calgary, Alberta, Canada, Can. J. Chem., 94, 414–423, https://doi.org/10.1139/cjc-2015-0426, 2016.

Morgan, W. T., Ouyang, B., Allan, J. D., Aruffo, E., Di Carlo, P., Kennedy, O. J., Lowe, D., Flynn, M. J., Rosenberg, P. D., Williams, P. I., Jones, R., McFiggans, G. B., and Coe, H.: Influence of aerosol chemical composition on N_2O_5 uptake: airborne regional measurements in northwestern Europe, Atmos. Chem. Phys., 15, 973–990, https://doi.org/10.5194/acp-15-973-2015, 2015.

Osthoff, H. D., Roberts, J. M., Ravishankara, A. R., Williams, E. J., Lerner, B. M., Sommariva, R., Bates, T. S., Coffman, D., Quinn, P. K., Dibb, J. E., Stark, H., Burkholder, J. B., Talukdar, R. K., Meagher, J., Fehsenfeld, F. C., and Brown, S. S.: High levels of nitryl chloride in the polluted subtropical marine boundary layer, Nat. Geosci., 1, 324–328, 2008.

Pathak, R. K., Wu, W. S., and Wang, T.: Summertime $PM_{2.5}$ ionic species in four major cities of China: nitrate formation in an ammonia-deficient atmosphere, Atmos. Chem. Phys., 9, 1711–1722, https://doi.org/10.5194/acp-9-1711-2009, 2009.

Pathak, R. K., Wang, T., and Wu, W. S.: Nighttime enhancement of $PM_{2.5}$ nitrate in ammonia-poor atmospheric conditions in Beijing and Shanghai: Plausible contributions of heterogeneous hydrolysis of N_2O_5 and HNO_3 partitioning, Atmos. Environ., 45, 1183–1191, https://doi.org/10.1016/j.atmosenv.2010.09.003, 2011.

Phillips, G. J., Tang, M. J., Thieser, J., Brickwedde, B., Schuster, G., Bohn, B., Lelieveld, J., and Crowley, J. N.: Significant concentrations of nitryl chloride observed in rural continental Europe associated with the influence of sea salt chloride and anthropogenic emissions, Geophys. Res. Lett., 39, 10.1029/2012GL051912, 2012.

Phillips, G. J., Thieser, J., Tang, M., Sobanski, N., Schuster, G., Fachinger, J., Drewnick, F., Borrmann, S., Bingemer, H., Lelieveld, J., and Crowley, J. N.: Estimating N_2O_5 uptake coefficients using ambient measurements of NO_3, N_2O_5, $ClNO_2$and particle-phase nitrate, Atmos. Chem. Phys., 16, 13231–13249, https://doi.org/10.5194/acp-16-13231-2016, 2016.

Riedel, T. P., Bertram, T. H., Crisp, T. A., Williams, E. J., Lerner, B. M., Vlasenko, A., Li, S. M., Gilman, J., de Gouw, J., Bon, D. M., Wagner, N. L., Brown, S. S., and Thornton, J. A.: Nitryl Chloride and Molecular Chlorine in the Coastal Marine Boundary Layer, Environ. Sci. Technol., 46, 10463–10470, 2012.

Riedel, T. P., Wagner, N. L., Dubé, W. P., Middlebrook, A. M., Young, C. J., Öztürk, F., Bahreini, R., VandenBoer, T. C., Wolfe, D. E., Williams, E. J., Roberts, J. M., Brown, S. S., and Thornton, J. A.: Chlorine activation within urban or power plant plumes: Vertically resolved $ClNO_2$ and Cl_2 measurements from a tall tower in a polluted continental setting, J. Geophys. Res.-Atmos., 118, 8702–8715, https://doi.org/10.1002/jgrd.50637, 2013.

Riemer, N., Vogel, H., Vogel, B., Anttila, T., Kiendler-Scharr, A., and Mentel, T. F.: Relative importance of organic coatings for the heterogeneous hydrolysis of N_2O_5 during summer in Europe, J. Geophys. Res.-Atmos., 114, D17307, https://doi.org/10.1029/2008JD011369, 2009.

Roberts, J. M., Osthoff, H. D., Brown, S. S., Ravishankara, A. R., Coffman, D., Quinn, P., and Bates, T.: Laboratory studies of products of N_2O_5 uptake on Cl^- containing substrates, Geophys. Res. Lett., 36, L20808, https://doi.org/10.1029/2009gl040448, 2009.

Ryder, O. S., Ault, A. P., Cahill, J. F., Guasco, T. L., Riedel, T. P., Cuadra-Rodriguez, L. A., Gaston, C. J., Fitzgerald, E., Lee, C., Prather, K. A., and Bertram, T. H.: On the Role of Particle Inorganic Mixing State in the Reactive Uptake of N_2O_5 to Ambient Aerosol Particles, Environ. Sci. Technol., 48, 1618–1627, https://doi.org/10.1021/es4042622, 2014.

Ryder, O. S., Campbell, N. R., Shaloski, M., Al-Mashat, H., Nathanson, G. M., and Bertram, T. H.: Role of Organics in Regulating $ClNO_2$ Production at the Air–Sea Interface, J. Phys. Chem. A, 119, 8519–8526, 2015.

Simon, H., Kimura, Y., McGaughey, G., Allen, D. T., Brown, S. S., Osthoff, H. D., Roberts, J. M., Byun, D., and Lee, D.: Modeling the impact of $ClNO_2$ on ozone formation in the Houston area, J. Geophys. Res.-Atmos., 114, D00F03, https://doi.org/10.1029/2008JD010732, 2009.

Simpson, W. R., Brown, S. S., Saiz-Lopez, A., Thornton, J. A., and v. Glasow, R.: Tropospheric Halogen Chemistry: Sources, Cycling, and Impacts, Chem. Rev., 115, 4035–4062, https://doi.org/10.1021/cr5006638, 2015.

Streets, D. G., Zhang, Q., Wang, L., He, K., Hao, J., Wu, Y., Tang, Y., and Carmichael, G. R.: Revisiting China's CO emissions after the Transport and Chemical Evolution over the Pacific (TRACE-P) mission: Synthesis of inventories, atmospheric modeling, and observations, J. Geophys. Res.-Atmos., 111, D14306, https://doi.org/10.1029/2006JD007118, 2006.

Su, X., Tie, X., Li, G., Cao, J., Huang, R., Feng, T., Long, X., and Xu, R.: Effect of hydrolysis of N_2O_5 on nitrate and ammonium formation in Beijing China: WRF-Chem model simulation, Sci. Total. Environ., 579, 221–229, 2017.

Sun, L., Xue, L., Wang, T., Gao, J., Ding, A., Cooper, O. R., Lin, M., Xu, P., Wang, Z., Wang, X., Wen, L., Zhu, Y., Chen, T., Yang, L., Wang, Y., Chen, J., and Wang, W.: Significant increase of summertime ozone at Mount Tai in Central Eastern China, Atmos. Chem. Phys., 16, 10637–10650, https://doi.org/10.5194/acp-16-10637-2016, 2016.

Tang, M. J., Telford, P. J., Pope, F. D., Rkiouak, L., Abraham, N. L., Archibald, A. T., Braesicke, P., Pyle, J. A., McGregor, J., Watson, I. M., Cox, R. A., and Kalberer, M.: Heterogeneous reaction of N_2O_5 with airborne TiO_2 particles and its implication for stratospheric particle injection, Atmos. Chem. Phys., 14, 6035–6048, https://doi.org/10.5194/acp-14-6035-2014, 2014.

Tham, Y. J., Yan, C., Xue, L., Zha, Q., Wang, X., and Wang, T.: Presence of high nitryl chloride in Asian coastal environment and its impact on atmospheric photochemistry, Chinese Sci. Bull., 59, 356–359, https://doi.org/10.1007/s11434-013-0063-y, 2014.

Tham, Y. J., Wang, Z., Li, Q., Yun, H., Wang, W., Wang, X., Xue, L., Lu, K., Ma, N., Bohn, B., Li, X., Kecorius, S., Größ, J., Shao, M., Wiedensohler, A., Zhang, Y., and Wang, T.: Significant concentrations of nitryl chloride sustained in the morning: investigations of the causes and impacts on ozone production in a polluted region of northern China, Atmos. Chem. Phys., 16, 14959–14977, https://doi.org/10.5194/acp-16-14959-2016, 2016.

Thornton, J. A., Kercher, J. P., Riedel, T. P., Wagner, N. L., Cozic, J., Holloway, J. S., Dubé, W. P., Wolfe, G. M., Quinn, P. K., Middlebrook, A. M., Alexander, B., and Brown, S. S.: A large atomic chlorine source inferred from mid-continental reactive nitrogen chemistry, Nature, 464, 271–274, 2010.

Wagner, N. L., Riedel, T. P., Young, C. J., Bahreini, R., Brock, C. A., Dubé, W. P., Kim, S., Middlebrook, A. M., Öztürk, F., Roberts, J. M., Russo, R., Sive, B., Swarthout, R., Thornton, J. A., VandenBoer, T. C., Zhou, Y., and Brown, S. S.: N_2O_5 uptake coefficients and nocturnal NO_2 removal rates determined from ambient wintertime measurements, J. Geophys. Res.-Atmos., 118, 9331–9350, https://doi.org/10.1002/jgrd.50653, 2013.

Wang, T., Ding, A. J., Gao, J., and Wu, W. S.: Strong ozone production in urban plumes from Beijing, China, Geophys. Res. Lett., 33, L21806, https://doi.org/10.1029/2006gl027689, 2006.

Wang, T., Tham, Y. J., Xue, L., Li, Q., Zha, Q., Wang, Z., Poon, S. C. N., Dubé, W. P., Blake, D. R., Louie, P. K. K., Luk, C. W. Y., Tsui, W., and Brown, S. S.: Observations of nitryl chloride and modeling its source and effect on ozone in the planetary boundary layer of southern China, J. Geophys. Res.-Atmos., 121, 2476–2489, https://doi.org/10.1002/2015jd024556, 2016.

Wang, T., Xue, L., Brimblecombe, P., Lam, Y. F., Li, L., and Zhang, L.: Ozone pollution in China: A review of concentrations, meteorological influences, chemical precursors, and effects, Scl. Total. Environ., 575, 1582–1596, 2017.

Wang, X., Wang, T., Yan, C., Tham, Y. J., Xue, L., Xu, Z., and Zha, Q.: Large daytime signals of N_2O_5 and NO_3 inferred at 62 amu in a TD-CIMS: chemical interference or a real atmospheric phenomenon?, Atmos. Meas. Tech., 7, 1–12, https://doi.org/10.5194/amt-7-1-2014, 2014.

Wang, X., Wang, H., Xue, L., Wang, T., Wang, L., Gu, R., Wang, W., Tham, Y. J., Wang, Z., Yang, L., Chen, J., and Wang, W.: Observations of N_2O_5 and ClNO2 at a polluted urban surface site in North China: High N_2O_5 uptake coefficients and low $ClNO_2$ product yields, Atmos. Environ., 156, 125–134, 2017.

Wang, Z., Wang, T., Gao, R., Xue, L., Guo, J., Zhou, Y., Nie, W., Wang, X., Xu, P., Gao, J., Zhou, X., Wang, W., and Zhang, Q.: Source and variation of carbonaceous aerosols at Mount Tai, North China: Results from a semi-continuous instrument, Atmos. Environ., 45, 1655–1667, 2011.

Wängberg, I., Barnes, I., and Becker, K. H.: Product and Mechanistic Study of the Reaction of NO_3 Radicals with α-Pinene, Environ. Sci. Technol., 31, 2130–2135, https://doi.org/10.1021/es960958n, 1997.

Wen, L., Chen, J., Yang, L., Wang, X., Caihong, X., Sui, X., Yao, L., Zhu, Y., Zhang, J., Zhu, T., and Wang, W.: Enhanced formation of fine particulate nitrate at a rural site on the North China Plain in summer: The important roles of ammonia and ozone, Atmos. Environ., 101, 294–302, 2015.

Wexler, A. S. and Clegg, S. L.: Atmospheric aerosol models for systems including the ions H^+, NH_4^+, Na^+, SO_4^{2-}, NO_3^-, Cl^-, Br^-, and H_2O, J. Geophys. Res.-Atmos., 107, ACH 14-11–ACH 14-14, https://doi.org/10.1029/2001JD000451, 2002.

Zhang, Q., Streets, D. G., Carmichael, G. R., He, K. B., Huo, H., Kannari, A., Klimont, Z., Park, I. S., Reddy, S., Fu, J. S., Chen, D., Duan, L., Lei, Y., Wang, L. T., and Yao, Z. L.: Asian emissions in 2006 for the NASA INTEX-B mission, Atmos. Chem. Phys., 9, 5131–5153, https://doi.org/10.5194/acp-9-5131-2009, 2009.

Zhou, Y., Wang, T., Gao, X. M., Xue, L. K., Wang, X. F., Wang, Z., Gao, J. A., Zhang, Q. Z., and Wang, W. X.: Continuous observations of water-soluble ions in $PM_{2.5}$ at Mount Tai (1534 m a.s.l.) in central-eastern China, J. Atmos. Chem., 64, 107–127, https://doi.org/10.1007/s10874-010-9172-z, 2009.